335

NATIONAL COOPERATIVE
HIGHWAY RESEARCH PROGRAM REPORT **335**

ACCEPTANCE CRITERIA FOR STEEL BRIDGE WELDS

TRANSPORTATION RESEARCH BOARD
NATIONAL RESEARCH COUNCIL

NATIONAL COOPERATIVE HIGHWAY RESEARCH PROGRAM REPORT **335**

ACCEPTANCE CRITERIA FOR STEEL BRIDGE WELDS

P. B. CROSLEY and E. J. RIPLING
Materials Research Laboratory, Inc.
Glenwood, Illinois

RESEARCH SPONSORED BY THE AMERICAN ASSOCIATION OF STATE HIGHWAY AND TRANSPORTATION OFFICIALS IN COOPERATION WITH THE FEDERAL HIGHWAY ADMINISTRATION

AREAS OF INTEREST

Structures Design and Performance
General Materials
(Highway Transportation, Public Transit, Rail Transportation)

TRANSPORTATION RESEARCH BOARD
NATIONAL RESEARCH COUNCIL
WASHINGTON, D.C.   DECEMBER 1990

NATIONAL COOPERATIVE HIGHWAY RESEARCH PROGRAM

Systematic, well-designed research provides the most effective approach to the solution of many problems facing highway administrators and engineers. Often, highway problems are of local interest and can best be studied by highway departments individually or in cooperation with their state universities and others. However, the accelerating growth of highway transportation develops increasingly complex problems of wide interest to highway authorities. These problems are best studied through a coordinated program of cooperative research.

In recognition of these needs, the highway administrators of the American Association of State Highway and Transportation Officials initiated in 1962 an objective national highway research program employing modern scientific techniques. This program is supported on a continuing basis by funds from participating member states of the Association and it receives the full cooperation and support of the Federal Highway Administration, United States Department of Transportation.

The Transportation Research Board of the National Research Council was requested by the Association to administer the research program because of the Board's recognized objectivity and understanding of modern research practices. The Board is uniquely suited for this purpose as: it maintains an extensive committee structure from which authorities on any highway transportation subject may be drawn; it possesses avenues of communications and cooperation with federal, state and local governmental agencies, universities, and industry; its relationship to the National Research Council is an insurance of objectivity; it maintains a full-time research correlation staff of specialists in highway transportation matters to bring the findings of research directly to those who are in a position to use them.

The program is developed on the basis of research needs identified by chief administrators of the highway and transportation departments and by committees of AASHTO. Each year, specific areas of research needs to be included in the program are proposed to the National Research Council and the Board by the American Association of State Highway and Transportation Officials. Research projects to fulfill these needs are defined by the Board, and qualified research agencies are selected from those that have submitted proposals. Administration and surveillance of research contracts are the responsibilities of the National Research Council and the Transportation Research Board.

The needs for highway research are many, and the National Cooperative Highway Research Program can make significant contributions to the solution of highway transportation problems of mutual concern to many responsible groups. The program, however, is intended to complement rather than to substitute for or duplicate other highway research programs.

NCHRP REPORT 335

Project 10-31 FY '86

ISSN 0077-5614

ISBN 0-309-04858-3

L. C. Catalog Card No. 90-71944

Price $7.00

NOTICE

The project that is the subject of this report was a part of the National Cooperative Highway Research Program conducted by the Transportation Research Board with the approval of the Governing Board of the National Research Council. Such approval reflects the Governing Board's judgment that the program concerned is of national importance and appropriate with respect to both the purposes and resources of the National Research Council.

The members of the technical committee selected to monitor this project and to review this report were chosen for recognized scholarly competence and with due consideration for the balance of disciplines appropriate to the project. The opinions and conclusions expressed or implied are those of the research agency that performed the research, and, while they have been accepted as appropriate by the technical committee, they are not necessarily those of the Transportation Research Board, the National Research Council, the American Association of State Highway and Transportation officials, or the Federal Highway Administration, U.S. Department of Transportation.

Each report is reviewed and accepted for publication by the technical committee according to procedures established and monitored by the Transportation Research Board Executive Committee and the Governing Board of the National Research Council.

Special Notice

The Transportation Research Board, the National Research Council, the Federal Highway Administration, the American Association of State Highway and Transportation Officials, and the individual states participating in the National Cooperative Highway Research Program do not endorse products or manufacturers. Trade or manufacturers names appear herein solely because they are considered essential to the object of this report.

Published reports of the

NATIONAL COOPERATIVE HIGHWAY RESEARCH PROGRAM

are available from:

Transportation Research Board
National Research Council
2101 Constitution Avenue, N.W.
Washington, D.C. 20418

Printed in the United States of America

FOREWORD

By Staff
Transportation Research Board

This report contains the findings of a study that was performed to develop improved acceptance criteria for bridge welds. In addition, the report documents an experimental research program that measured fatigue crack growth rates under stress spectra realistic for highway bridges. Existing literature and research results were examined in an attempt to define acceptance criteria that would ensure repair of harmful discontinuities in welds (imperfections which would cause fatigue failures), while preventing unnecessary repairs. This report provides a comprehensive description of the research along with recommended criteria intended for inclusion in the ANSI/AASHTO/AWS D1.5 *Bridge Welding Code.* The contents of this report will be of immediate interest and use to bridge engineers, welding and materials engineers, steel bridge fabricators, specification writing bodies, researchers, and others concerned with the design, fabrication, and inspection of welded steel bridge components.

The use of inaccurate methods of nondestructive evaluation and empirical acceptance criteria for bridge welds has resulted in unnecessary repair of welds and has permitted unsound welds to be incorporated in some bridges. Failure to apply accurate bridge weld quality acceptance criteria can significantly increase construction and maintenance costs or can lead to structural failures. Weld repairs can generate harmful residual stresses and distortions and can often create new and more serious discontinuities.

Radiographic and ultrasonic weld-quality accpetance standards currently in use for bridge welds had their origin in the boiler and pressure vessel industry. Use of these empirical standards has been justified by the inherent inaccuracy of nondestructive test methods. With improvements in the ability of nondestructive tests to measure and characterize flaws, it is appropriate to develop better weld quality acceptance criteria. The development of new criteria based on appropriate analytical methods and verification procedures can produce realistic bases for design and inspection decisions. Such weld criteria should produce safer bridge welds while reducing unnecessary repairs.

NCHRP Project 10-31, Acceptance Criteria for Steel Bridge Welds, was initiated with the objective of developing needed improvements in bridge weld acceptance criteria. The research entailed collecting and evaluating existing literature and data, and performing analytical studies and laboratory testing to develop new data. This report documents the work performed under Project 10-31.

During the course of the study, the technology for weld inspection and weld flaw quantification was also under development and improvement in a number of research projects around the world. Therefore, it was the intent of this project that these emerging technologies play an important role in the improved acceptance criteria.

Expected improvements in weld inspection and weld flaw quantification technology were not available in a timely manner to the researchers on this study. Therefore, the acceptance criteria developed under Project 10-31 were based on existing, inaccurate inspection and quantification methods. The criteria are sufficiently flexible, however, so that they can be adjusted and improved as technology permits in the future.

It should also be noted that the technical recommendations resulting from this report have not received universal endorsement by experts in this field. Such disagreement on technical issues and recommendations should, however, stimulate discussion between fracture mechanics experts resulting in additional advances in the future. In the meantime, the criteria recommended in this report could provide incremental advances in the state of the art of steel bridge weld fabrication, inspection, and acceptance.

CONTENTS

ACKNOWLEDGMENTS

The research reported herein was performed under NCHRP Project 10-31 by the Materials Research Laboratory, Inc. P. B. Crosley was the Principal Investigator and E. J. Ripling was Co-Principal Investigator. Much of the testing was carried out by Russ Janota.

Consultants W. D. Doty, G. J. Hill, P. E. Masters, and C. E. Thunman, Jr., contributed to the planning of the research effort; and G. J. Hill gave invaluable help in making welds with deliberately introduced imperfections. The authors wish to acknowledge the constructive comments of the NCHRP Project Panel which provided guidance throughout the course of the project.

ACCEPTANCE CRITERIA FOR STEEL BRIDGE WELDS

SUMMARY

The objective of this research was to develop improved weld acceptance criteria for steel bridge welds. To the extent possible with current technology, and anticipating potential improvements in nondestructive test methods, the acceptance criteria should result in the repair of welds containing harmful discontinuities, that is, weld imperfections which would cause fatigue failures. At the same time the criteria should not mandate unnecessary weld repairs.

On the basis of fracture mechanics analysis and experimental fatigue studies, allowable imperfection sizes for different effective stress ranges are suggested. These findings can potentially be used with any nondestructive testing methods which define weld imperfection size. In this report, revisions to the current weld acceptance criteria in the area of radiographic and magnetic particle inspection are proposed. The major change involves taking the design stress range, F_{sr}, into account in specifying acceptable weld imperfection sizes. This recognizes the fact that stress range is a crucial factor in determining whether or not an imperfection will develop into a fatigue failure. Other changes involve removing the current dependence of acceptable imperfection size on thickness (effective weld throat) and revising the conditions under which neighboring discontinuities are considered to be interactive. Inspection requirements for ultrasonic examination are left unchanged because the inspection procedure does not give an adequate characterization of weld imperfections to support specific modifications.

The reasoning behind the proposed changes in weld acceptance criteria is based on a fracture mechanics evaluation of imperfections based on treating them as sharp cracks, and supporting experimental studies. The experimental portion of the program consisted of two phases. The first was measurement of fatigue crack growth rates (da/dN) under a stress spectrum realistic for highway bridges and with ΔK in the range 1.5 to 10 ksi$\sqrt{\text{in.}}$, the appropriate range as defined in the fracture mechanics analysis. The second part of the experimental study involved an investigation of the development of fatigue cracks from deliberately introduced weld discontinuities, porosity, and slag inclusions.

CHAPTER ONE

INTRODUCTION AND RESEARCH APPROACH

OVERVIEW

A harmful weld imperfection is one that leads to a fatigue failure; a harmless one is one that does not develop into a fatigue crack or, if it does, the crack growth is so limited as to be of no consequence for structural performance. Ideally, weld acceptance criteria would identify all harmful imperfections and require their repair, while all harmless imperfections would be accepted. This is an unattainable ideal.

This project was conceived at a time when significant advances in imperfection characterization were anticipated, and it was hoped that these would be the basis on which to build more rational weld acceptance criteria. The expected improvements in evaluation of weldments by using ultrasonic testing did not materialize. Even if they had, it would not be possible to discriminate, with a high degree of certainty, between harmful and harmless imperfections. It is more realistic to deal with the probability, P, that an imperfection may be harmful, and to analyze the factors that enter into this probability. For example, in a situation where there were 1,000 seemingly identical imperfections in apparently equivalent fluctuating stress environments, it is not likely that all 1,000 would lead to a fatigue failure by a given time, or that none would. Most probably some fraction, P, would prove to be harmful while the remainder, $1 - P$, would prove harmless. Of course, P will be near zero for small imperfections and low stress fluctuations, and near unity for large discontinuities and higher stresses. It would be simpler if P were always either zero or one, but this cannot generally be expected, and the best that can be hoped for is a reliable estimate of P.

Suppose a weld imperfection were judged to have a 5 percent probability of being harmful, that is, $P = 0.05$. Should it be repaired? This kind of question can be addressed in a formal manner. If, for example, the cost of repairing a fatigue failure that might result from the imperfection were 20 times the cost of removing the initial imperfection, economic considerations alone indicate that the imperfection should be repaired. Accepting this conclusion, however, means acknowledging at the outset that many harmless imperfections may have to be removed in order to eliminate one harmful one. This is an inescapable feature of any rational weld acceptance criteria.

The work carried out on this project included analytical and experimental studies designed to clarify the factors affecting the probability, P, that a weld imperfection may be harmful. One can write

$$P = P(\Delta\sigma_{eff}, a, q) \tag{1}$$

which is an abbreviated way of saying that the probability, P, depends on three factors or groups of factors. $\Delta\sigma_{eff}$ is the effective stress range in the region of the imperfection, a is a measure of the size of the imperfection, and q is a catch-all of leftover factors such as the shape of the imperfection, its orientation, edge sharpness, and so on. These factors will be treated in detail in subsequent chapters of the report, but at this point some general observations or assertions can be made.

Whether or not an imperfection will become a fatigue origin, and, if so, how fast the fatigue cracking will progress, depend strongly on the magnitude of the stress fluctuations in the region of the imperfection. $\Delta\sigma_{eff}$ is an important factor in Eq. 1, and any weld acceptance criteria based on a realistic assessment of whether or not an imperfection may be harmful must take stress range into account. The current weld acceptance criteria in the *Bridge Welding Code* (*1*) make no reference to stress range. Although it is recognized that there are practical obstacles to doing so, it will be recommended in this report that stress range considerations will be incorporated into the weld acceptance criteria.

When the stress distribution in a material is interrupted by a discontinuity, stress intensification does not, of course, develop uniformly over the remaining cross section; it occurs primarily in the immediate vicinity of the discontinuity. Therefore, it is the absolute size of an imperfection, the factor a in Eq. 1, that controls an imperfection's potency as a fatigue origin, and not its size relative to the dimensions of the cross section. In the current weld acceptance criteria (*1*) the acceptable discontinuity size is scaled to the thickness, that is, the groove weld effective throat. In the weld acceptance criteria to be proposed in this report, acceptable discontinuity size will not depend on thickness.

Another factor affecting the probability that an imperfection is harmful is its proximity to other imperfections or to an edge; and, in this area, some changes from current weld acceptance criteria are also proposed.

In general, the recommendations made in this report are aimed at replacing current empirical radiographic weld quality acceptance standards, with standards based on assessment of the probability that a particular discontinuity will be the origin of a fatigue failure. Although the probabilities cannot be precisely defined, the procedure is a step in the direction of producing more realistic bases for design and inspection decisions. The proposed weld quality criteria should help produce safer bridges while reducing unnecessary repairs.

RESEARCH APPROACH

Linear elastic fracture mechanics deals with sharp cracks. For this type of discontinuity it provides a basis for relating the first two factors in Eq. 1, $\Delta\sigma_{eff}$, and a. To do this it defines an effective stress intensity factor range, ΔK_{eff}, which has a determinate dependence on $\Delta\sigma_{eff}$ and a. In applying linear elastic fracture mechanics to discontinuities in bridges, it was noted that virtually all of the data on fatigue crack growth pertained to ΔK_{eff} greater than 10 ksi$\sqrt{\text{in.}}$, whereas the area of interest was ΔK_{eff} ranging downward from 10 ksi$\sqrt{\text{in.}}$ to, perhaps, 2 ksi

$\sqrt{in.}$ or less. Thus, an experimental study was undertaken to measure fatigue crack growth rates at low ΔK_{eff} on plates of AASHTO M222 and M244 steels (ASTM A588 and A514, respectively).

Any imperfection which proves to be the origin of a fatigue failure in a bridge or other structure will at some time develop into a sharp crack and extend as a sharp crack; and an investigation of fatigue crack growth is obviously relevant. On the other hand, detected imperfections that are ascertained to be cracks are not allowed by current standards, and it will not be proposed here that they be accepted. Of immediate concern in weld acceptance criteria are fusion defects such as porosity, entrapped slag, incomplete fusion. The experimental program also involved, therefore, an investigation of fatigue behavior of weld samples containing deliberately introduced slag inclusions and porosity.

To be meaningful, the fatigue studies had to be carried out under a stress spectrum realistic for highway bridges. This meant, not only that the crack growth rate studies would involve near-threshold crack extension rates, but also that the weld imperfection studies would involve fatigue lives of the order of tens of millions of cycles. The program was extended in time by one year to accommodate this testing; but, even so, only a limited number of tests could be run. Given the inherently probabilistic nature of the information being dealt with, it is necessary to be cautious about drawing too firm a conclusion from a small number of tests, especially in the case of the "natural" discontinuities.

The point of the program, of course, is to use the experimental data, and any other available information, to devise rational—and practical—weld acceptance criteria. The fatigue crack growth rate studies, based on linear elastic fracture mechanics, can be made into a tidy analytical package. Unfortunately, the real weld imperfections of interest are not, at least initially, sharp cracks. On the other hand, a unified analytical approach accounting for the geometrical variety of "natural" discontinuities is scarcely to be expected. The approach taken here, therefore, has been to use the fracture mechanics analytical model to arrive at weld acceptance criteria, and then determine whether the results on weld imperfections invalidate the model or suggest changes in it. In doing this it should be kept in mind that with respect to any particular imperfection detected in nondestructive examination there are three uncertainties. First, the imperfection will not be accurately characterized in terms of its size and shape; second, the fluctuating stresses that will be operative cannot be precisely known; and third, given a precise characterization of the imperfection and the stress environment, it is not possible to predict with certainty the subsequent fatigue behavior. Within the constraints imposed by these uncertainties, it is still appropriate to seek the most rational weld acceptance criteria.

CHAPTER TWO

FINDINGS

ANALYTICAL STUDIES

A weld imperfection may be thought of as a region which cannot support a tensile stress. Fluctuating tensile stresses that would otherwise have been transmitted through the imperfection are now transferred to adjacent material, where the increased stress range may initiate a fatigue failure. The magnitude and distribution of the stress intensification that occurs in the vicinity of an imperfection will depend on the nominal stress level (and stress range), and on the size of the imperfection; they will also depend on the general shape of the imperfection, on its orientation in the stress field, and on the sharpness of its edges. Analytical procedures that would take into account all of these variables and lead to a prediction of their combined effect on fatigue life are not available. Even if such procedures were available, the inability of nondestructive examination to characterize flaws fully would limit their usefulness in deciding whether or not to accept a particular imperfection discovered in the weld inspection.

Fracture mechanics is concerned with sharp cracks. By itself, therefore, fracture mechanics cannot take into account an imperfection's edge sharpness, and some general shapes of flaws cannot be realistically handled. When an imperfection can be treated as a sharp crack (which is always the case in the crack growth phase, if not the initiation, of a fatigue failure), fracture mechanics provides some tremendous unifying simplifications. Most importantly, it defines the relationship between imperfection size and stress level or stress range. It can also account for the effect of flaw orientation.

In linear elastic fracture mechanics the stress state at the leading edge of a sharp crack is characterized by a parameter, K, known as the stress intensity factor. The stress intensity factor is related to applied stress, σ, and crack size, a, by an expression of the type

$$K = Y\,\sigma\,(\pi a)^{1/2} \tag{2}$$

where Y is a dimensionless shape factor which depends on the configuration under consideration. In general, the factor Y can itself depend on the crack size, but for cases of interest here it can be assumed that $Y = 1$. Under a fluctuating stress with a range $\Delta\sigma$ the stress intensity factor range is

$$\Delta K = Y\,\Delta\sigma\,(\pi a)^{1/2} \tag{3}$$

Application of fracture mechanics to fatigue involves experimental determination of the crack growth rate per cycle, da/dN, as a function of the stress intensity factor range ΔK. The dependence of da/dN on ΔK is often expressed by a power law relationship

Table 1. Fatigue behavior of sharp cracks of different sizes at different stress ranges.

a. Initial ΔK for different combinations of crack size and stress range:

		Initial ΔK (ksi√in) for				
	2a=	1/16	1/8	1/4	1/2	1 inch
Effective stress range, $\Delta\sigma_{eff}$ (ksi)	8	2.51	3.54	5.01	7.09	10.03
	6	1.88	2.66	3.76	5.32	7.52
	4.5	1.41	1.99	2.82	3.99	5.64
	3	0.94	1.33	1.88	2.66	3.76
	2	0.63	0.89	1.25	1.77	2.51

b. Cyclic life for different combinations of crack size and stress range:

		Millions of cycles for crack to double in size for				
	2a=	1/16	1/8	1/4	1/2	1 inch
Effective stress range, $\Delta\sigma_{eff}$ (ksi)	8	1.19	0.97	0.79	0.64	0.52
	6	2.52	2.05	1.67	1.35	1.10
	4.5	5.33	4.33	3.52	2.86	2.32
	3	15.31	12.43	10.10	8.20	6.66
	2	43.92	35.68	28.98	23.54	19.12

$$da/dN = C\,(\Delta K)^n \tag{4}$$

where C and n are constants determined to fit a set of crack growth measurements. If there is a level of ΔK below which $da/dN = 0$, that level is referred to as a fatigue crack growth threshold.

Table 1a shows values of ΔK for selected combinations of stress range, $\Delta\sigma$, and crack size, 2a. Five values of $\Delta\sigma$ extend from 2 ksi to 8 ksi, a realistic range for steel highway bridges. Five crack size values span a 16-fold range from 2a = $\frac{1}{16}$ in. to 2a = 1 in. The values of ΔK are simply calculated from Eq. 3 taking $Y = 1$, and the table has been set up so as to give roughly constant values of ΔK along diagonals from upper left to lower right. First, it may be noted that the ΔK values thus calculated are almost all substantially less than 10 ksi$\sqrt{\text{in.}}$, and this defines the area of interest for crack growth rate studies in this program. Second, Table 1a illustrates the importance of stress range as a factor in fatigue; a two-fold change in $\Delta\sigma$ has the same effect on ΔK as a four-fold change in crack size. This is simply because $\Delta\sigma$ enters Eq. 3 linearly, whereas a enters as a square root. The implication for weld acceptance criteria is that having a good definition of stress range is at least as important as having a good definition of imperfection size in assessing whether an imperfection will be a harmful one or not.

FATIGUE BEHAVIOR OF SHARP CRACKS

Fatigue crack growth rate measurements at low ΔK were made on AASHTO M222 and M244 steels (ASTM A588 and A514). The tests used a spectrum load based on the same distribution proposed and used by Schilling and Klippstein (*2*) and later used by Fisher (*3*). Stress ratios of $R = 0.9$ and higher were used to mimic the effects of possible tensile residual stresses, and to avoid the possibly misleading crack closure influences. Testing details and more complete results are given in Appendix C. A summary of the results is given in Figure 1. The line plotted in the figure corresponds to Eq. 4 with $n = 2.6$ and $C = 1.5(10)^{-9}$

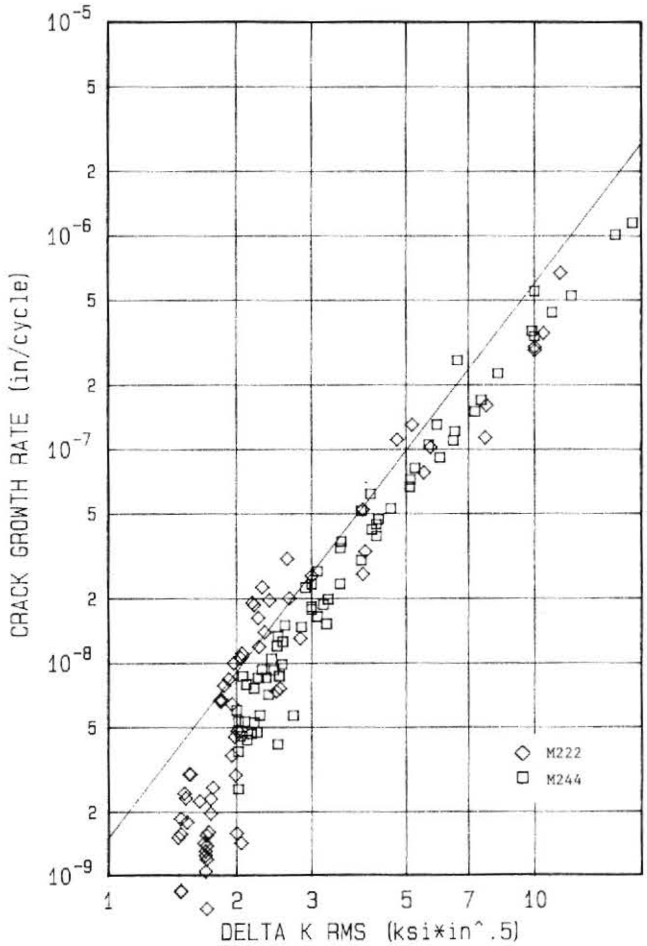

Figure 1. Fatigue crack growth rate measurements on M222 and M244 steels.

(for da/dN in inch/cycle and ΔK in ksi$\sqrt{\text{inch}}$). The ΔK is the root-mean-square value for the spectrum used. This line, while not strictly an upperbound, is a generally conservative representation of the results. Crack growth was detected at ΔK as low as 1.5 ksi$\sqrt{\text{in.}}$, but below about 2.5 ksi$\sqrt{\text{in.}}$ there is a departure from the linear relationship toward lower crack growth rates.

It is a straightforward exercise to combine Eqs. 3 and 4 and integrate between two crack length limits to obtain the number of fatigue cycles required for that amount of crack growth. Table 1b shows the result of such calculations for the same conditions represented in Table 1a. The results are given in terms of the number of stress cycles required to produce a doubling of the crack size. For example, at $\Delta\sigma_{eff}$ = 8 ksi, 1.19 million cycles are required for a crack to grow from 2a = $\frac{1}{16}$ in. to 2a = $\frac{1}{8}$ in., then another 970,000 cycles are required for the crack to grow to 2a = $\frac{1}{4}$ in., and so on.

There is a significant contrast between Table 1a and Table 1b. In terms of initial ΔK, positions along a diagonal in Table 1a represent roughly equivalent conditions; in terms of remaining fatigue life, this is definitely not the case. For two cracks having at some point the same ΔK, a large crack under a low stress range provides a significantly greater remaining life than does a short crack under a high stress range. In other words, when crack growth is taken into account, the already strong influence of stress range becomes even more pronounced. It is probably quite safe to say that primary protection against fatigue failure comes about because stress fluctuations are generally low, rather than because weld imperfections are controlled.

FATIGUE BEHAVIOR OF NATURAL IMPERFECTIONS

Weldments in 1-in. thick plates of AASHTO M222 (ASTM A588) and of M244 (A514) steel with deliberately introduced porosity and entrapped slag were fabricated, and axial fatigue specimens with a 1-in. square cross section were machined from them. A total of eight specimens, four from each steel type, were tested. The tests employed the same load spectrum used in the fatigue crack growth rate tests. The stress ratios were lower, $R = 0.5$ and $R = 0.33$, because of limited test machine capacity. The root-mean-square stress ranges were chosen, based on radiographic evaluation of the imperfections, to produce failure in about 5 million cycles based on crack growth rate performance.

Details are given in Appendix C; the results are summarized in Table 2. Of the eight specimens tested, three failed under the initial spectrum loading conditions. The remaining five were still intact after 30 to 50 million load cycles; and to induce failures in these specimens a constant amplitude high stress range loading was employed. (Stress ranges not marked "rms" in Table 2 are constant amplitude.) When the specimens were finally broken the fracture surfaces could be examined to determine (1) the actual size and shape of the imperfection at which fatigue cracking originated and (2) whether or not, in the specimens which did not fail under the low amplitude spectrum loading, any cracking occurred in the initial fatigue phase.

Even when imperfections were fully exposed on the fracture surfaces of the tested specimens, it was not always easy to identify the appropriate a dimension to use in a fracture mechanics analysis. In most cases, however, a reasonable estimate could be made; and the initial ΔK values given in Table 2 are based on assessment of discontinuities on the fracture surfaces. The estimated initial ΔK values ranged from 2.25 to 3.7 ksi $\sqrt{\text{in.}}$ It was also observed that four of the five specimens, which did not completely fail in the initial low amplitude load spectrum, did show evidence of fatigue cracking originating at imperfections in the fracture surface. The behavior is more fully documented in Appendix D; an example is given here. Figure 2 shows the fracture surface of specimen A588/D. Three imperfections of approximately the same size are apparent on the fracture surface; two of the three show evidence of fatigue cracking in the initial low amplitude spectrum loading.

Table 2. Axial fatigue testing of specimens with weld imperfections.

Specimen	Stress Range (kip)	Stress Ratio, R[1]	Millions of Cycles	Initial ΔK^2 (ksi/in)	Result
A514/S1	6.5 rms	0.50	29.59	3.20	failed
A514/S2	5.5 rms	0.50	25.00	3.70	failed
A514/P1	6.5 rms	0.50	29.59	2.80	crack(?)
	9.0 rms	0.25	9.57	--	crack
	27.0	0.10	1.47	--	failed
A514/P2	6.5 rms	0.50	33.78	3.60	no crack
	18.0	0.10	4.74	--	no crack
	27.0	0.10	1.54	--	failed
A588/A	8.0 rms	0.33	51.32	2.50	crack
	25.0	0.10	0.58	--	failed
A588/B	8.0 rms	0.33	52.25	3.20	crack
	27.0	0.10	0.90	--	failed
A588/C	8.0 rms	0.33	7.00	2.25	failed
A588/D	8.0 rms	0.33	50.51	2.25	crack
	22.5	0.10	5.51	--	crack
	27.0	0.10	5.56	--	failed

[1] The loading pattern consisted of a base load, P_0, and a fluctuating load, P_{rms}. The stress ratio is $R = P_0 / (P_0 + P_{rms})$.

[2] The initial ΔK is the root-mean-square stress intensity factor calculated from the rms stress and the initial imperfection size as measured on the fracture surface.

Looking at the totality of the data summarized in Table 2 and assessing it relative to what might have been expected based on the numbers in Table 1 suggests the following. In all eight specimens the cyclic lives were always greater than would have been expected from the sharp crack model, and, usually, many times greater. While five specimens survived upward of about 40 million cycles, four of the five showed evidence that fatigue cracking was underway; they would not have survived indefinitely. In other words, controlling imperfection size such that the initial ΔK is of the order of 2.5 ksi $\sqrt{\text{in.}}$ will probably result in quite long fatigue lives, but clearly does not guarantee immunity from fatigue failure.

CHAPTER THREE

INTERPRETATION, APPRAISAL, APPLICATIONS

The findings presented in the preceding chapter have been concerned primarily with the influence of discontinuity size and stress range on fatigue performance. In order to incorporate this information into weld acceptance criteria it is necessary to consider how well an imperfection can be characterized by nondestructive examination, how accurately the stress range can be predicted, and other factors that may influence whether or not an imperfection may be harmful, that is, lead to a fatigue failure. These issues will be considered here.

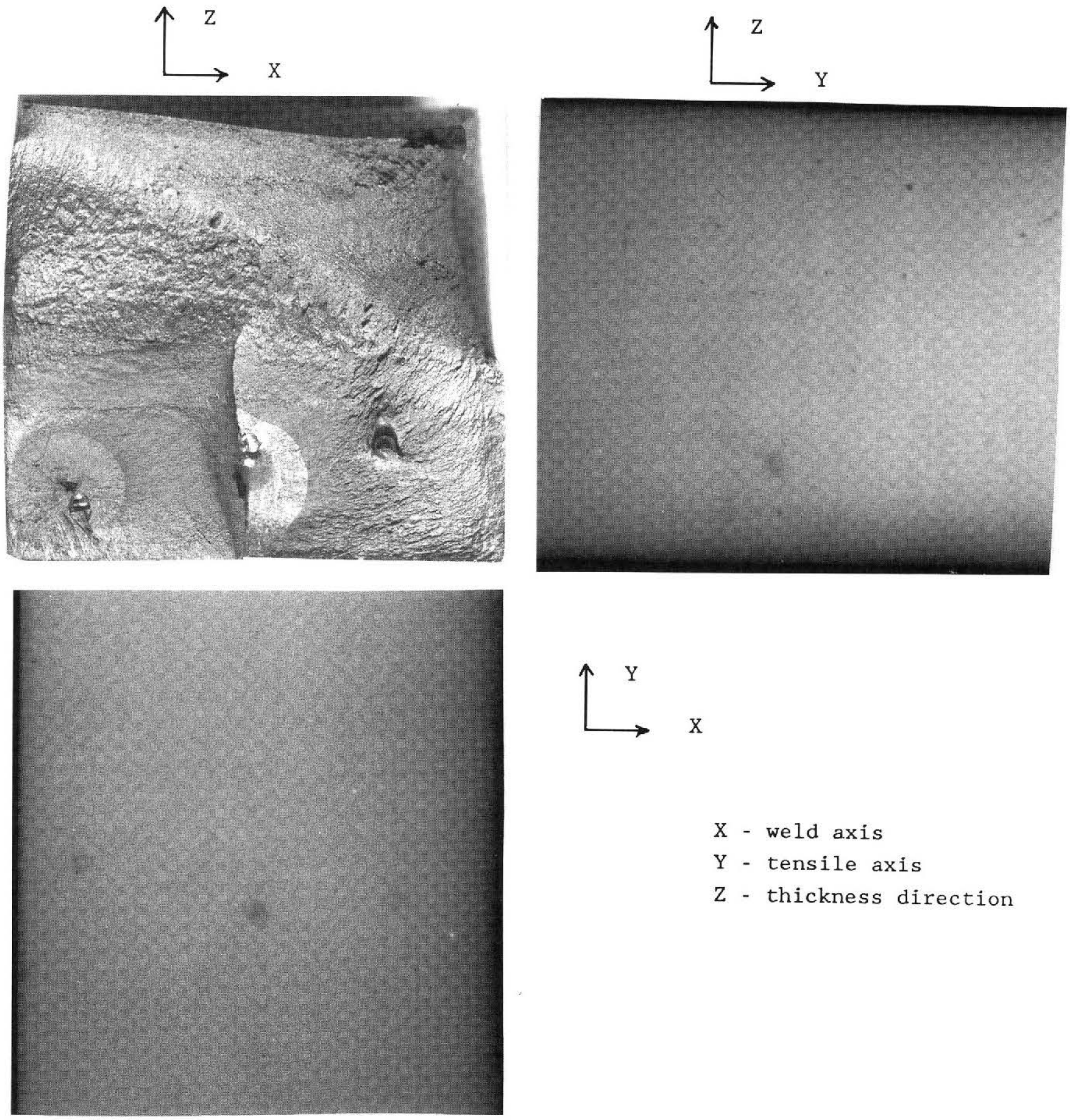

Figure 2. Documentation of fatigue testing of specimen A588/D. The fracture plane contains three distinct, isolated imperfections all of about the same size, approximately 0.05 in. across. Two appear to be fatigue origins and show clear evidence of crack growth in the initial variable amplitude loading, 50.5 million cycles at $\Delta\sigma_{rms}$ of 8 ksi. The third does not appear to have been of fatigue origin. Imperfection size corresponds to an initial ΔK_{rms} of about 2.25 ksi $\sqrt{in.}$

INSPECTION

Sophisticated ultrasonic techniques hold the greatest promise for more complete weld imperfection characterization, but present procedures do not give adequate definition upon which to base rational weld acceptance criteria. When commercially practical techniques are available, they can be incorporated readily into the framework of the proposed weld acceptance criteria. In this report it seems appropriate to concentrate on other inspection methods. Information provided by radiographic testing (RT) and by surface inspection methods (VT, MT, PT) is limited, but the limitations are easy to understand. Thus, the greatest potential for this program is with weld acceptance standards based on these tests; and RT will be treated here.

Views A, B, and C in Figure 3 represent three projections of a groove weld containing an imperfection, *d*, The most informative view from a fracture mechanics viewpoint is projection C; it defines the dimension 2α which is the critical dimension for fracture or fatigue. A radiograph provides only projection A; it allows definition of a dimension, $2a$, the trace of the imperfection normal to the principal stress direction. If one calculates a stress intensity value with the formula $K = \sigma(\pi a)^{1/2}$, this implies an assumed imperfection as shown in view C′, that is, an imperfection extending uniformly across the weld throat. If the imperfection were circular, as in view C″, the stress intensity factor would be $K = (2/\pi)\sigma(\pi a)^{1/2}$, that is, less than ⅔ the value for configuration C′. (This assumes, however, that the imperfection is not near enough to the top or bottom surfaces to feel their influence.) Weld imperfections will commonly be as small or smaller in the thickness direction than along the weld axis. In this case, because the smaller dimension predominates in determining the stress intensity factor, K, or its range ΔK, the radiograph does not provide information about the most critical dimension. (This is precisely the deficiency that the time-of-flight technology was expected to remedy.)

Taking the stress intensity factor to be $K = \sigma(\pi a)^{1/2}$ where $2a$ is simply the trace of the imperfection projected perpendicular to the normal stress direction is a conservative simplification. In the case where $2a$ is significantly larger than the thickness direction dimension of the discontinuity and where the discontinuity is well removed from the top or bottom surfaces, it may be absurdly overconservative. The benefits of the simplification, however, outweigh the drawbacks of this conservatism. First of all, there is no practical way to evaluate the thickness direction dimension. Secondly, on the assumption that it is considerably more costly to repair a fatigue failure than to remove a weld imperfection, it is prudent to repair imperfections which may have only a small probability of being harmful. Finally, the acceptance criteria need not be concerned with the through the thickness location of the discontinuity (the worst case has been assumed); the same acceptance standards, therefore, can be applied to surface evaluations (VT, MT, PT) as to radiographic evaluation.

By reducing a three-dimensional problem to a two-dimensional problem, the issue of interacting discontinuities can be readily evaluated. In a repeated array of equal length cracks, the stress intensity factor increases by a factor of $\sqrt{2}$ when the distance between neighboring cracks is reduced to about ¼ of the crack length. In other words, the stress fields of discontinuities do not interact significantly unless they are quite close together. For practical purposes, therefore, considering distances measured perpendicular to the normal stress direction (that is, along with the weld axis in Figure 2), if an imperfection of length $2a$ is at a distance greater than $2a$ from an edge or from another imperfection, it can be regarded as an isolated imperfection.

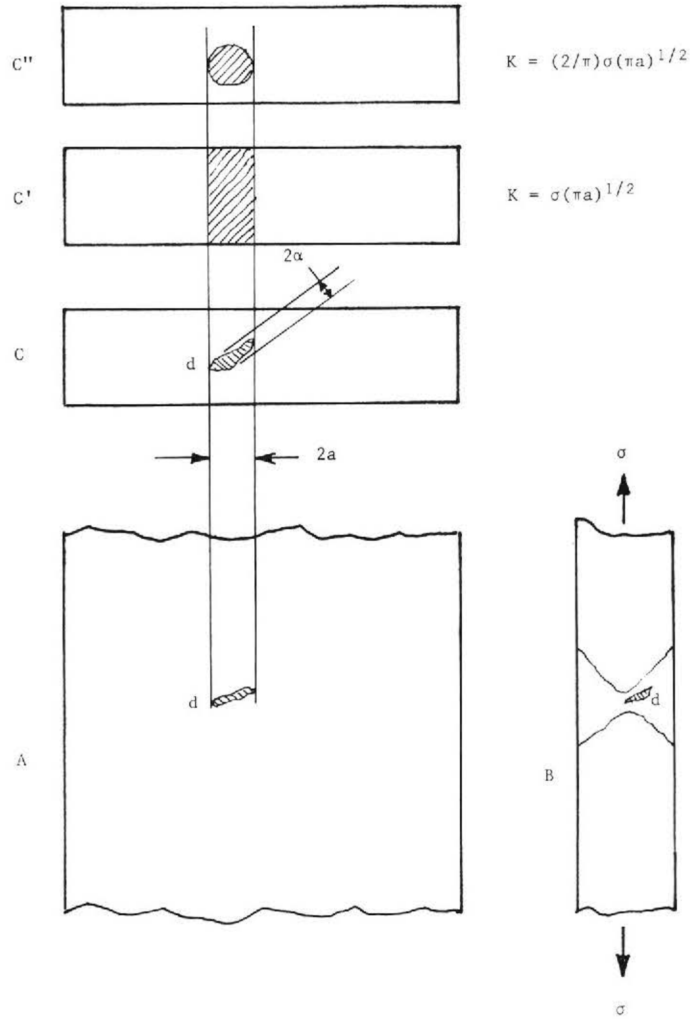

Figure 3. Characterization of the geometry of weld imperfections.

STRESS RANGE

As emphasized in the introductory chapter, the effective stress range, denoted $\Delta\sigma_{eff}$, is a crucial factor in determining whether or not an imperfection will develop into a fatigue failure. In practice, an accurate definition of $\Delta\sigma_{eff}$ will not be available; the design parameter closest to $\Delta\sigma_{eff}$ is the design stress range, F_{sr}. Formally at least, F_{sr} can be any value from, perhaps, 2 ksi, up to a maximum of 16 ksi for a Category B detail. Presumably, $\Delta\sigma_{eff}$ could vary from case to case by the same proportion. It is not possible, with this level of uncertainty in effective stress range, to devise weld acceptance criteria based on a realistic assessment of whether or not an imperfection may be harmful. Different acceptance criteria are needed for different stress ranges.

One way to obtain an estimate of $\Delta\sigma_{eff}$ is to assume it has a fixed relationship to the design stress range F_{sr}; and, in the absence of better information, a reasonable assumption may be $\Delta\sigma_{eff} = 0.5\ F_{sr}$, that is, that the root-mean-square value of the bridge load spectrum is about one-half the design calculated maximum value. (Here and throughout the report F_{sr} does *not* refer to the design *allowable* stress range, but rather to the value actually calculated in the course of verifying that the maximum allowable is not exceeded. For example, the allowable value of $F_{sr} = 16$ ksi will seldom govern for a Category B detail; the actual calculated value will be smaller. It is, of course, the actual value that is relevant for fatigue; and, hence, the value designated by F_{sr} in this report.) This is consistent with the spectrum used in the experimental phase of this program, but not necessarily valid for a particular steel bridge.

WELD ACCEPTANCE CRITERIA

Table 1, introduced in the chapter on findings, showed calculated values of ΔK and of cyclic life for different combinations of stress range, $\Delta\sigma$, and crack length, $2a$. At this point it is a matter of going from precise mathematical definitions of $\Delta\sigma$ and $2a$ to simplified practical definitions usable in weld acceptance criteria. The translations have already been suggested: $2a$ will be taken as the projection perpendicular to the normal stress direction of an NDE indication, specifically a VT, MT, PT, or RT indication. The $\Delta\sigma_{eff}$ will be taken as one-half the design stress range, F_{sr}. It seems reasonable to follow Table 1 and use increments of discontinuity size that change by a factor of two. For roughly constant ΔK this corresponds to stepping F_{sr} by a factor of about $\frac{3}{2}$, and five categories are needed to span a complete range of F_{sr} and cover an appropriate range of imperfection size. It is proposed that the diagonal elements of Table 1, that is, the condition that $\Delta K = 2.5\ \text{ksi}\sqrt{\text{in.}}$, approximately, be taken as the acceptance standard. Thus, the proposed weld acceptance criteria are as follows:

Maximum F_{sr}:	16	12	9	6	4 ksi
Discontinuity size:	1/16	1/8	1/4	1/2	1 inch

It is acknowledged that there may be practical difficulties in applying, in effect, five different standards. In particular, who tells an inspector which standard is to be applied to a particular weld? One possibility is to include the statement, "Unless otherwise specified, a value for F_{sr} of 9 ksi shall be assumed." The rationale behind this statement is that, in general, F_{sr} will be below 9 ksi; and it seems reasonable, from a workmanship point of view, to repair discontinuities greater than $\frac{1}{4}$ in.

The above table considers the size of individual imperfections, but does not address the questions of imperfection clusters. This can be handled with the statement, "When the clearance between adjacent imperfections is less than the length of either one, the pair shall be considered to be a single discontinuity." This is somewhat more stringent than a fracture mechanics analysis might require, but is much more lenient than the current weld quality requirements.

Specific recommendations for incorporating the proposed acceptance criteria into the *Bridge Welding Code, ANSI/AASHTO/AWS D1.5-88* are given in Appendix A.

CHAPTER FOUR

CONCLUSIONS AND SUGGESTED RESEARCH

CONCLUSIONS

Determining whether or not a particular weld discontinuity will become the origin of a fatigue failure requires information of three types: a characterization of the discontinuity, a prediction of the stress spectrum to which the discontinuity will be subjected, and, finally, the experience to say how such a discontinuity under such stresses will behave in fatigue. There are significant uncertainties in each of these areas.

The area most seriously neglected by the current weld acceptance criteria is effective stress spectrum; and the weld acceptance criteria proposed here attempt to improve this by specifying different standards for different levels of design stress range, F_{sr}. Making this change does not imply that the stress spectrum is closely predictable, but simply that some consideration has to be given to this factor to have any hope of predicting fatigue performance.

The proposed acceptance criteria are based on judgments which take the different uncertainties into account; but they are not uniquely correct. They should certainly be subject to revision whenever pertinent information becomes available. It should be borne in mind, however, that even the best imaginable information will not allow unequivocal prediction of whether or not a particular discontinuity will develop into a growing fatigue crack. The best that can ever be done is to establish a reliable estimate of the probability that an imperfection will lead to a failure.

More quantitative assessment of the probability that a discontinuity will be harmful requires (1) a prediction of the fluctuating stresses in the region encompassing the discontinuity, (2) the capability to characterize the discontinuity by nondestructive inspection, and (3) experimental data on the potency of weld imperfections as fatigue origins.

Prediction of Stresses

The probability that an imperfection is harmful is strongly dependent on the stress range; and a procedure for predicting the effective stress range should be incorporated into weld acceptance criteria. The proposed criteria assume that the effective stress range is about one-half the design stress range, F_{sr}; but it would be highly desirable to have a better established correlation.

Obviously, it will not be possible to predict precisely the fluctuating stresses that a weld in a future bridge will experience; and a tight correlation between F_{sr} and effective stress may not exist. Stress spectrum information obtained from instrumentation of existing bridges, and examination of calculated stress ranges in relation to this information, could enhance the capability of predicting effective stress ranges under anticipated traffic conditions.

Characterization of Imperfections

Neither surface inspection procedures nor radiography define the thickness direction dimension of an imperfection, and the weld acceptance criteria proposed here are based on using the incomplete information provided by these methods. Ultrasonic inspection offers the possibility of more complete flaw size description. When more advanced UT techniques reach the stage of practical inspection tools, they can be readily incorporated into the proposed weld acceptance criteria offered here. Better flaw characterization will enhance the ability to predict the probability that an imperfection is harmful, and, hence, will provide more discriminating weld acceptance criteria.

Weld Imperfections as Fatigue Origins

More information on the fatigue behavior of weld imperfections would be desirable. Because it is not clear how discontinuity size and stress range interact for imperfections other than sharp cracks, data should be collected on realistic weld imperfections at the low effective stress ranges expected in bridges. This entails testing to large numbers of load cycles. Moreover, tests of this type show large variabilities in cyclic life; and, therefore, a statistical approach is required both in assessing the data and in applying it to bridges. Obtaining enough test data to be statistically significant could be a very costly undertaking.

RECOMMENDED RESEARCH

Each of the three topics considered above is concerned with controlling fatigue failures in bridges; and the issue of controlling fatigue goes well beyond the topic of weld acceptance criteria. It is important, for example, not just to repair weld discontinuities that are deemed to be harmful, but to keep the total population of weld imperfections as low as practically possible. Moreover, protection against fatigue relies more on controlling effective stress ranges than on eliminating weld flaws.

Research in each of the three areas would be desirable, and is justifiable on the basis of contributing more to the larger issue of fatigue control, rather than to the limited one of developing better weld acceptance criteria. The weld acceptance criteria proposed here provide the framework into which new information or new capabilities in any of the three areas can readily be incorporated. The authors would not recommend, therefore, any new program directed toward weld acceptance criteria *per se*. The authors would hope, however, that work in all three areas would continue in the expectation that findings would influence design and welding practice.

REFERENCES

1. AMERICAN WELDING SOCIETY, *Bridge Welding Code ANSI/ AASHTO/AWS D1.5-88.* (1988) p. 220.
2. KLIPPSTEIN, K. H., and SCHILLING, C. G., "Stress Spectrums for Short-Span Steel Bridges." *Fatigue Crack Growth under Spectrum Loads, ASTM STP 595* (May 1976) pp. 203–216.
3. FISHER, J. W., MERTZ, D. R., and ZHONG, A., "Steel Bridge Members Under Variable Amplitude Long Life Fatigue Loading." *NCHRP Report 267,* (Dec. 1983) p. 26.
4. AMERICAN WELDING SOCIETY, *Structural Welding Code, Steel, ANSI/AWS D1.1-86* (Feb. 1986) p. 356.
5. NEWMAN, J. C., JR., "Crack Opening Displacements in Center-Crack, Compact, and Crack-Line Wedge-Loaded Specimens." *NASA Technical Note NASA TN D-8268* (July 1976).
6. ROLFE, S. T., and BARSOM, J. M., *Fracture and Fatigue Control in Structures.* Prentice-Hall, Englewood Cliffs, N.J. (1977).

APPENDIX A

PROPOSED WELD ACCEPTANCE CRITERIA

Incorporating the weld acceptance criteria proposed here would involve rather modest editorial changes to the Bridge Welding Code[1]. Quality of Welds is addressed in section 9.25, and the major subdivisions are: 9.25.1 Visual Inspection, 9.25.2 Radiographic and Magnetic Particle Inspection, 9.25.3 Ultrasonic Inspection, and 9.25.4 Liquid Penetrant Inspection.

9.25.1 Visual Inspection

No changes recommended.

9.25.2 Radiographic and Magnetic Particle Inspection

9.25.2.1 For welds in redundant members subject to tensile stress under any condition of loading, the projected length of any porosity or fusion type discontinuity that is 1/16 in (1.6 mm) or longer shall not exceed the size, B, indicated in Table 9.25.2.1.

TABLE 9.25.2.1

Weld quality requirements for discontinuities occurring in tension welds in redundant members (limitation of porosity and fusion type discontinuities):

Design stress range, F_{sr} (ksi) :	16	12	9	6	4
Projected discontinuity length, B (in) :	1/16	1/8	1/4	1/2	1

Note 1: Projected discontinuity length is the length of the radiographic or magnetic particle indication projected onto a line perpendicular to the primary stress direction.

Note 2: When F_{sr} is not specified, F_{sr} = 9 ksi shall be assumed.

9.25.2.2 For welds in fracture critical non-redundant members subject to tensile stress under any condition of loading the projected length of any porosity or fusion type discontinuity that is 1/16 in (1.6 mm) or longer shall not exceed the size, B, indicated in Table 9.25.2.2.

TABLE 9.25.2.2

Weld quality requirements for discontinuities occurring in tension welds in non-redundant members (limitation of porosity and fusion type discontinuities):

Design stress range, F_{sr} (ksi) :	12	9	6	4
Projected discontinuity length, B (in) :	1/16	1/8	1/4	1/2

Note 1: Projected discontinuity length is the length of the radiographic or magnetic particle indication projected onto a line perpendicular to the primary stress direction.

Note 2: When F_{sr} is not specified, F_{sr} = 9 ksi shall be assumed.

Note 3: When F_{sr} exceeds 12 ksi, the projected discontinuity length shall not exceed 1/16 inch; however, it is desirable to keep F_{sr} below 12 ksi.

9.25.2.3 For welds subject to compressive stress only and specifically indicated as such on the design drawings, neither radiographic nor magnetic particle inspection are required.

9.25.2.4 When the distance from any porosity or fusion type discontinuity described above to another such discontinuity is less than the projected length of the larger, the two shall be treated as a single discontinuity. The projected length of the combined single discontinuity is taken as the projected length of the two together.

9.25.2.5 When the separation distance from any porosity or fusion type discontinuity to an edge or to the toe or root of any intersecting flange-to-web weld is less than the projected length of the discontinuity, the effective projected length of the discontinuity shall be deemed to be twice the sum of the length of the discontinuity plus the separation distance.

9.25.3 Ultrasonic Inspection

No changes recommended.

9.25.4 Liquid Penetrant Inspection

No changes recommended.

APPENDIX B

COMMENTARY ON PROPOSED CRITERIA

Weld acceptance criteria serve two purposes, to preserve workmanship standards and to provide protection against failure. Protecting against failure involves eliminating harmful weld imperfections, specifically those that may prove to be fatigue origins. Ideally, all harmful imperfections would be repaired and all harmless ones would be accepted. Even under these ideal conditions, workmanship standards would still be important. Rather than requiring repair of harmful imperfections, it would be better that they not exist in the first place. When it is acknowledged that distinguishing harmful from harmless imperfections entails substantial uncertainty, it is even more important to minimize the imperfection population by requiring high standards of workmanship. Under the current weld acceptance criteria, the require- ments specified under Visual Inspection are primarily workmanship standards, and no changes in them are proposed. Liquid penetrant inspection, which may be regarded as an extension of visual inspection, is likewise left unaltered.

Ultrasonic examination has, perhaps, the potential to become a precise tool for imperfection characterization; but it is not so at present. The viewpoint taken here, therefore, is that ultrasonic inspection in the current criteria is, in effect, a workmanship standard; and changes to the current criteria are not recommended.

Radiographic and magnetic particle examination provide incomplete but readily interpretable information about imperfection size; and in this area substantial changes are recommended. The most radical change is the scaling of allowable imperfection size with the design stress range, F_{sr}. This recognizes the fact that stress range is an influential factor in determining whether or not a discontinuity will develop into a fatigue crack. In contrast to the current criteria, imperfection size is not scaled to thickness (effective weld throat). First, it is the absolute size of an imperfection, not its size relative to the cross section, that determines its potency as a fatigue origin. Second, the inspection tools (RT and MT) do not evaluate the through-the-thickness dimension of the discontinuity, anyway. Another proposed change involves the evaluation of groups of discontinuities; the proposed changes recognize the fact that the stress fields of neighboring imperfections do not interact unless the imperfections are quite close.

The proposed Table 9.25.2.1 is meant to require repair of discontinuities which have more than a small probability of developing into a fatigue crack, or of extending very rapidly if they do. There is not enough information to assess what this probability is; and, even with the use of different acceptance standards for different levels of F_{sr}, the probability of fatigue failure will remain greater in the high F_{sr} region of operation. Higher stress ranges inherently mean a greater probability of fatigue failure; and this fact cannot be wholly compensated for by a sliding scale of weld acceptance standard.

Since the consequences of a fatigue failure are more serious in a non-redundant member than in a redundant one, it is appropriate to use the weld acceptance criteria to obtain lower probability of fatigue failure, that is, to repair still more harmless imperfections in order to get rid of some harmful ones. Thus Table 9.25.2.2 is shifted by one category relative to Table 9.25.2.1. This, however, presents a difficulty. It is not practical to eliminate discontinuities with dimensions less than 1/16 inch; yet imperfections of this size have some probability of developing into fatigue failures, especially with F_{sr} in the 12 to 16 ksi range. In other words, in order to have a high degree of protection against fatigue failure, the appropriate action is to control F_{sr}, not to rely on eliminating minuscule weld imperfections.

In practice, values of F_{sr} in excess of 9 ksi are probably rarely encountered; maximum stress rather than stress range governs design for Category B and even Category C weld details. It is probably reasonable to assume, in the absence of information to the contrary, that F_{sr} is less than 9 ksi, and a note to this effect is appended to the proposed Tables 9.25.2.1 and 9.25.2.2.

APPENDIX C

EXPERIMENTAL PROGRAM

The experimental program consisted of two parts. The first was measurement of fatigue crack growth rates in AASHTO M222 and M244 (ASTM A588 and A514 steels) at low ΔK. The second involved fatigue tests on welds containing deliberately introduced imperfections. The same variable amplitude load spectrum was used in both parts of the program.

STRESS SPECTRUM

The variable amplitude loading pattern involved indefinitely repeating the same 1000-cycle block. The block used sixteen equally spaced load amplitude levels. The number of cycles at each load level was based on the truncated Rayleigh distribution devised by Klippstein and Schilling[2] and subsequently employed by Fisher et al.[3]. The distribution of load ranges is shown in Fig. C-1. A random number generation scheme was used to select the order of occurrence of the cycles within the block. All of the cycles had the same minimum load; the amplitude variation was made up in the load maximum, as shown in Fig. C-2. To characterize the amplitude of an entire 1000-cycle block the root-mean-square (rms) value was selected. The rms load translates to a range in stress intensity factor, ΔK_{rms}, and the minimum load to K_{min}. The stress ratio, R, is given by

$$R = K_{min}/(K_{min} + \Delta K_{rms}) \tag{C-1}$$

and a crack tip loading condition for a 1000-cycle block is completely characterized by a value of ΔK_{rms} and R. (In the da/dN ranges of interest in this program the crack growth occurring in a single 1000-cycle block is too small to have a measurable effect on ΔK_{rms} under a fixed rms load.)

It was assumed originally that the maximum testing frequency would be realized if the period of a cycle was in direct proportion to its amplitude. With this relationship it turned out that the low amplitude cycles were attenuated before the higher amplitude ones were affected. The software was modified accordingly to lengthen preferentially the lower amplitude cycles. It was hoped that an effective frequency of 20 Hertz could be maintained. This proved to be too fast at shorter crack lengths where higher loads are required, but a rate near 20 Hertz was attainable at longer crack lengths. Two test machines were run under the same computer program. The mean load and load amplitude were separately adjustable for each machine, but both had to be run at the same frequency. Thus the machine/specimen combination requiring the lower frequency determined the testing rate.

CRACK GROWTH RATE TESTS

Test Specimens

The crack growth rate specimens, as shown in Fig. C-3, were standard compact specimens of ASTM Standard E647 with W = 8 inches and B = 1 inch. The computer calculation of crack length was based on the compliance versus crack length evaluations given by Newman[5]. An expression fitted to the Newman data is as follows:

$$1-a/W = 61.0238\ X^4 - 42.2022\ X^3 + 6.8043\ X^2 + 3.19505\ X + 0.0278197 \quad \text{(C-2)}$$

where a is the crack length, W is the specimen width, and X is a non-dimensional compliance given by

$$X = EB(2V)/P \quad \text{(C-3)}$$

where E is Young's modulus, B is specimen thickness, 2V is the crack opening at the specimen edge, and P is the load. The computer would read 2V and P at the peak and trough of a load cycle, and used these in the above equation to calculate 1-a/W and hence a.

Test Procedure

The testing of each da/dN specimen involved two phases. The first consisted of a stepwise decrease in ΔK_{rms} from the value at which the crack could be initiated from a machined notch down to threshold level magnitudes. At the same time the stress ratio, R, was increased from near-zero to the high value of interest. (The reason for concern with fatigue crack growth at high R was based on the reasoning that a high R would simulate the possible deleterious effect of tensile residual stresses. In addition, testing at high R should minimize crack closure effects which could produce a lower cracking rate in the da/dN test than might be present under actual bridge conditions.) The second phase of the testing of a da/dN specimen was the growth of the crack at a constant rms load and stress ratio from the threshold condition through the usable crack length range of the specimen. It was possible, of course, to collect da/dN data during the first phase of stepwise decreasing ΔK_{rms} as well as in the second phase.

Test Results

Crack growth data obtained on two specimens of AASHTO M244 (ASTM A514) steel are reproduced here, in the form of a log-log plot, in Fig. C-4. For both specimens the constant rms load portion of the testing was begun when ΔK_{rms} had been reduced to 2 ksi$\sqrt{in}$, and the stress ratio was R = 0.9. This level of ΔK_{rms} does not in any sense represent a threshold, but merely the level below which measurements were not attempted. In both specimens da/dN dependence on ΔK_{rms} was the same in the increasing ΔK phase of the testing as it had been during the stepwise reduction phase.

Straight lines on the log-log plot correspond to a relationship between the crack growth rate per cycle, da/dN, and the stress intensity range, ΔK, described by a power law equation

$$da/dN = C \, [(\Delta K)/(\Delta K)_0]^n \qquad \text{(C-4)}$$

where $(\Delta K)_0$ is a reference stress intensity factor range, and C and n are constants.[1] In this report, $(\Delta K)_0$ will be taken as 1.0 ksi$\sqrt{\text{in}}$. Two reference lines are plotted on Fig. C-4. The lower, labeled F-P, corresponds to $n = 3$ and $C = 3.6(10)^{-10}$ in/cycle. This relationship, based on da/dN measurements on ferrite-pearlite steels at ΔK generally above 10 ksi$\sqrt{\text{in}}$, predicts a crack growth rate somewhat lower than was observed. The second reference line (M), with $n = 2.25$ and $C = 6.6(10)^{-9}$ in/cycle, is based on data from martensitic steels. It predicts crack growth rates significantly greater then those measured on the M244 steel specimens.

The test results from two specimens of AASHTO M222 (ASTM A588) steel are presented in Fig. C-5. The same reference lines, F-P and M, are also reproduced here. In these test more attention was given to exploring the threshold region, ΔK_{rms} in the range 1.5 to 2 ksi$\sqrt{\text{in}}$. Some crack growth was observed at ΔK_{rms} as low as 1.5 ksi$\sqrt{\text{in}}$ in one specimen and 1.7 ksi$\sqrt{\text{in}}$ in the other; but when it was attempted to start the constant rms load cycling from these levels crack extension remained at or below 10^{-9} in/cycle, and at times appeared to have stopped. Increasing the stress ratio from 0.91-0.92 to about 0.94-0.95 seemed to have no effect in increasing da/dN, and finally the rms load on each specimen was increased by about ten percent in order to get crack growth started again. When the testing was resumed it was noted, in both specimens, that the da/dN values were somewhat larger than the values obtained in the stepwise decreasing phase of the tests. Although the increase, of the order of a factor of two, is within the scatter commonly observed in da/dN measurements; it seemed rather suspect that the same deviation should occur at the same time in two different specimens. A satisfactory physical explanation was never found.

The crack growth rate measurements made on the M222 and M244 steels are plotted together in Fig. C-6. Also plotted is a curve used to represent the data; this curve corresponds to eq. (C-4) with the constants $n = 2.6$ and $C = 1.5(10)^{-9}$ in/cycle, and thus lies about midway between the curves F-P and M in the preceding figures. This curve was originally selected as an upper bound to the data collected on M222 and M244 steels; all of the data points lying above the curve are from the increasing ΔK portion M244 tests. Although no longer strictly an upper bound, the relationship is a reasonable, somewhat conservative, representation of the crack growth measurements made in this study.

---

[1] By explicitly including $(\Delta K)_0$ in the equation, the constant, C, takes on a physical meaning: it's the crack growth rate at $\Delta K = (\Delta K)_0$, and it has the same units as da/dN. This makes mathematical sense, too, because the quantity raised to the power <u>n</u> is really a dimensionless ratio.

Comparison with Existing Data

Very few da/dN data at ΔK less than 10 ksi$\sqrt{in}$ are available; however, Fisher et al[3] made measurements on AASHTO M183 (ASTM A36) steel. Their results are shown in Fig. C-7. An obvious difference is that the da/dN measurements of Fisher on M183 steel are consistently below the ferrite-pearlite reference line whereas the MRL data on M222 and M244 are consistently above it. The difference is not great and is consistent with the variability in crack growth rates obtained at higher ΔK. At the same time it is surprising that the data on M244 and M222, one a quenched and tempered steel and the other not, should agree so closely while the results on M183 are distinctly different. It might be noted that Fisher used a root-mean-cube value to characterize the load (or K) spectrum while we have used the root-mean-square, but the difference is less than ten percent.[2] The two investigators have, of course, used different discrete approximations to the continuous Rayleigh distribution function, and some subtle spectrum effect may have been operative.

The data of Fisher on M183 steel show downward deviations from the power law representation at ΔK levels which depend on the stress ratio, R. At the highest stress ratio, R = 0.8, there is the suggestion of a threshold at ΔK of about 2.3 ksi$\sqrt{in}$, and no data were obtained with ΔK below this level. In this program, on the other hand, fatigue crack growth rates were measured down to 2 ksi$\sqrt{in}$ in M244 steel and 1.5 ksi$\sqrt{in}$ on M222 steel with R = 0.9. There is some downward deviation from the power law representation at ΔK of 1.5 to 2 ksi$\sqrt{in}$ as can be seen in Fig. C-6 where the da/dN data from both steels are plotted. Taken together, the Fisher data and the MRL data are consistent in indicating that threshold type behavior is displaced toward lower ΔK as the stress ratio, R, is increased. Perhaps, with a still higher stress ratio, the power law relations might extend to still lower ΔK.

[2]The rms value is about 0.46 of the maximum value of the continuous truncated Rayleigh distribution; the rmc value is about 0.50 times the maximum.

Significance

Crack growth rate data of the type shown in Figs. C-4 to C-6 can be used in a quantitative way to predict fatigue life. The basic integration is

$$N = \int_{a_i}^{a_f} da/(da/dN) \qquad \text{(C-5)}$$

where N is the number of stress cycles required for a crack to grow from a size a_i to a size a_f. Equation (C-4) provides an expression for da/dN, and the data on M222 and M244 steels provide the constants $C = 1.5(10)^{-9}$ in/cycle and n = 2.6. This fit <u>may</u> be unrealistically conservative at ΔK below 2 ksi$\sqrt{in}$, and it <u>may</u> be unrealistically conservative at higher ΔK for lower stress ratios. In the case of highway bridges it is prudent, however, to assume a high stress ratio even if the applied stresses correspond to a low R. First, local tensile residual stresses could produce an effective high R in a region encompassing the crack. Second, a sharp tipped non-planar discontinuity might not benefit from crack closure effects which may account for some or all of the apparent threshold behavior at low R. Consequently, in carrying out the integration of eq. (C-5) it is appropriate to use the power law relationship and not anticipate threshold behavior.

The last information needed to carry out the integration of eq. (C-5) is the relationship between the stress intensity range (ΔK), the stress range ($\Delta\sigma$), and crack size. For this we use the wide plate formula

$$\Delta K = (\Delta\sigma)\ (\pi a)^{1/2} \qquad \text{(C-6)}$$

This is a reasonable expression for an interior crack oriented perpendicular to the stress field as long as the leading edges of the crack do not approach a free surface. Under these assumptions <u>a</u> is the crack half-length (or half the minor axis of an elliptical crack).

Carrying out the indicated integration leads to the following expression:

$$N = [a_i/(kC)]\ [(\Delta K)_0/(\Delta K)_i]^n\ [1-(a_i/a_f)^k] \quad \text{(C-7a)}$$

where

$$(\Delta K)_i = (\Delta\sigma)\ (\pi a_i)^{1/2} \quad \text{(C-7b)}$$

and

$$k = (n/2) - 1 \quad \text{(C-7c)}$$

These equations were used to construct Table 1. First eq. (C-7b) was used to determine values of $(\Delta K)_i$ for various combinations of effective stress range $\Delta\sigma = \Delta\sigma_{eff}$ and initial crack length, a_i. This constitutes Table 1a. Then, for the same combinations of $\Delta\sigma$ and a_i, eq. (C-7a) was used to calculate N for crack growth from a_i to $a_f = 2.a_i$. This constitutes Table 1b.

FATIGUE OF WELD IMPERFECTIONS

Specimen Preparation

Two complete penetration groove welds joining one-inch thick plate sections of AASHTO M244 (ASTM A514) steel were prepared. One weld had deliberately introduced slag inclusions, and the other porosity. Each of the welds, which were about ten inches long, was x-rayed; and, based on the radiographs, locations from which to machine tension-tension axial fatigue specimens were selected. Two specimens were obtained from the weldment with entrapped slag (A514/S1 and A514/S2), and two from the weldment containing porosity (A514/P1 and A514/P2). The specimens, as shown in Fig. C-8, had square cross-sections, one-inch by one-inch. This size was chosen as a compromise between having a specimen as large as possible and staying within the loading capacity of the available test machines.

Similar specimens were prepared from one-inch plate sections of AASHTO M222(ASTM A588) steel. The only difference was that, based on the experience with the other material, more attention was given to producing single, isolated imperfections. These weldments yielded four specimens, A588/A, A588/B, A588/C, and A588/D.

Test Procedure

Having specimens with a one inch square cross section made it possible to x-ray the welds in two perpendicular directions, a luxury not available in RT inspection of a full length of weld in a bridge. Having two views of the imperfections made it possible to gage their size, and the stress ranges for the axial fatigue tests were chosen so as to produce failures in five to ten million cycles based on the da/dN test results. The imperfection size estimated for specimen A514/S2 was

2a = 0.25 inch, and the stress range selected was $\Delta\sigma_{rms}$ = 5.5 ksi. Specimens A514/S1, A514/P1, and A514/P2 were estimated to have effective crack sizes of the order of 2a = 0.125 inch and were tested at $\Delta\sigma_{rms}$ = 6.5 ksi. For A588/A, A588/C and A588/D the estimated 2a was 0.05 inch, and $\Delta\sigma_{rms}$ was 8 ksi, as it was for specimen A588/B where the initial estimated 2a was only about 0.03 inch. It may be noted that with respect to Table 1, the conditions chosen for the tests represent positions close to the diagonal and toward the high stress range end of the table.

Because of the high load ranges associated with the peak cycles in the stress spectrum, it was not possible to run these tests at the very high stress ratios (0.9 and greater) used in the da/dN tests; and a stress ratio of R = 0.5 was selected.

Initially the tests were interrupted every five million or so cycles, and specimens were x-rayed in the hope of detecting some evidence of crack extension from the imperfections. The radiographs did not reveal anything, and this practice was discontinued.

It was originally planned to section run-out specimens, and look for metallographic evidence of cracking in the vicinity of the discontinuities located in the radiographs. In the end it was decided, instead, to continue the testing at an elevated stress range in the hope that examination of the fracture surfaces would reveal how far fatigue cracking had progressed at the time of the load change. This worked very well.

Results

The test results are summarized in Table 2; and Figs. C-9 through C-16 show the fracture surfaces and radiographs of each of the specimens.

Out of the eight specimens tested, only three failed under the originally imposed stress spectrum. Specimen A588/C failed after 7.00 million stress cycles, the expected life based on the da/dN data. Specimens A514/S2 and A514/S1 failed after 25 and 29.59 million cycles, respectively. As Table 2 shows, the remaining five specimens had not failed after 30 to 50 million cycles under the original spectrum loading, and failed only under constant amplitude load cycling at very much higher stress ranges. Examination of the fracture surfaces, however, indicated that four of the five had developed cracks in the original cycling.

Imperfections which were the origin of fatigue cracking can be measured directly on the fracture surfaces. In general, their shapes are somewhat irregular; and selecting a size to be associated with the crack length, 2a, used in a fracture mechanics calculation involves some uncertainty. Nevertheless, estimates were made and values for initial

ΔK_{rms} were made. The values are indicated in Table 2. Curiously, a specimen with an initial ΔK_{rms} = 2.25 ksi$\sqrt{in}$, lowest in the group of eight specimens, failed in the shortest time.

Given the values of initial ΔK_{rms}, the cyclic lives generally exceeded what might be expected based on the da/dN measurements. Specimen A588/C was an exception; all the others had long fatigue lives presumably because some amount of stress cycling was absorbed in sharpening the discontinuities. In seven out of eight cases, however, some cracking did occur; and the specimens would ultimately have failed in fatigue.

<u>Significance</u>

A sample of eight specimens does not constitute a statistically significant number of tests, in view of the variability in the tests and the even greater variability of fatigue conditions in actual bridges. The results of the tests are in no way alarming; they suggest that actual imperfections are in general less severe fatigue origins than sharp cracks. At the same time the tests are not sufficient to quantify any additional margin of safety. In general, if the imperfection population in a bridge is controlled such that those with an initial ΔK_{eff} of more than about 2.5 ksi$\sqrt{in}$ are eliminated, long fatigue lives should in general result. But immunity from fatigue cannot be guaranteed.

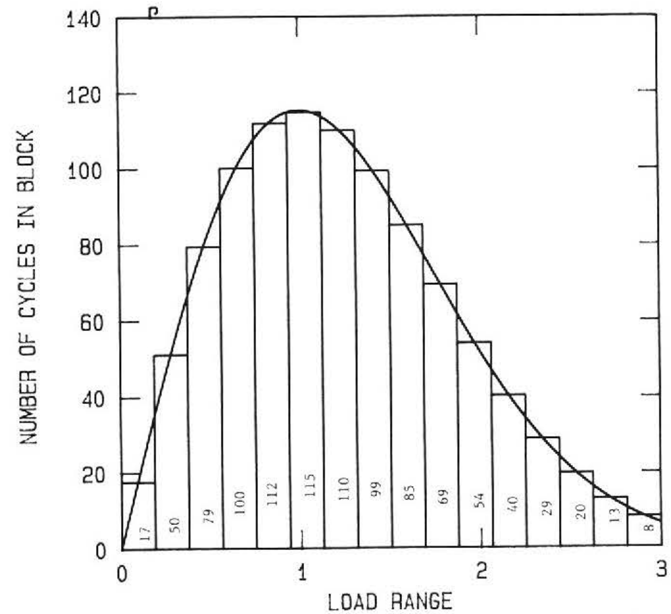

Fig. C-1. Histogram fitted to truncated Rayleigh distribution showing number of cycles at each load level in 1000-cycle block.

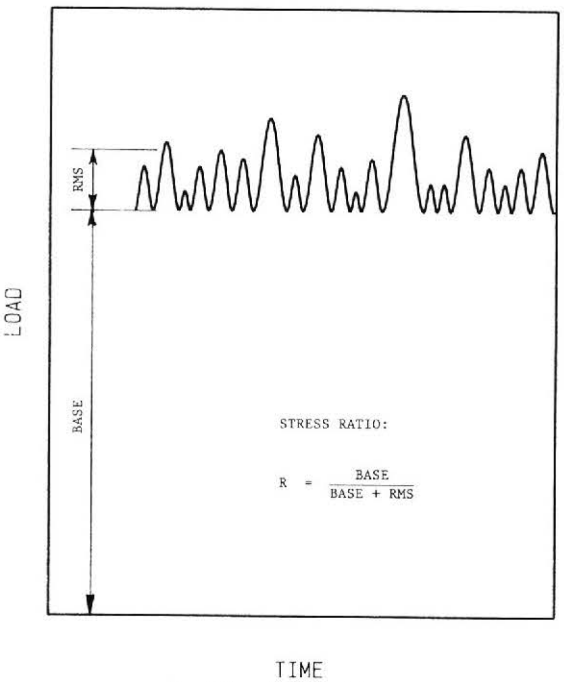

Fig. C-2. Segment of 1000-cycle variable amplitude load block.

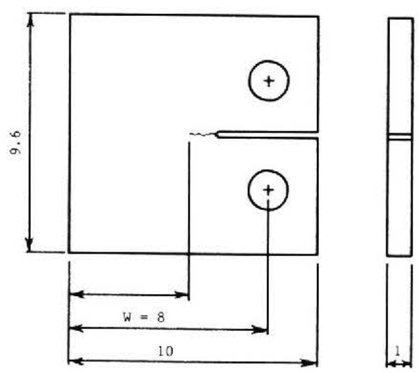

Fig. C-3. Compact specimen used to measure fatigue crack growth rates. (Dimensions in inches.)

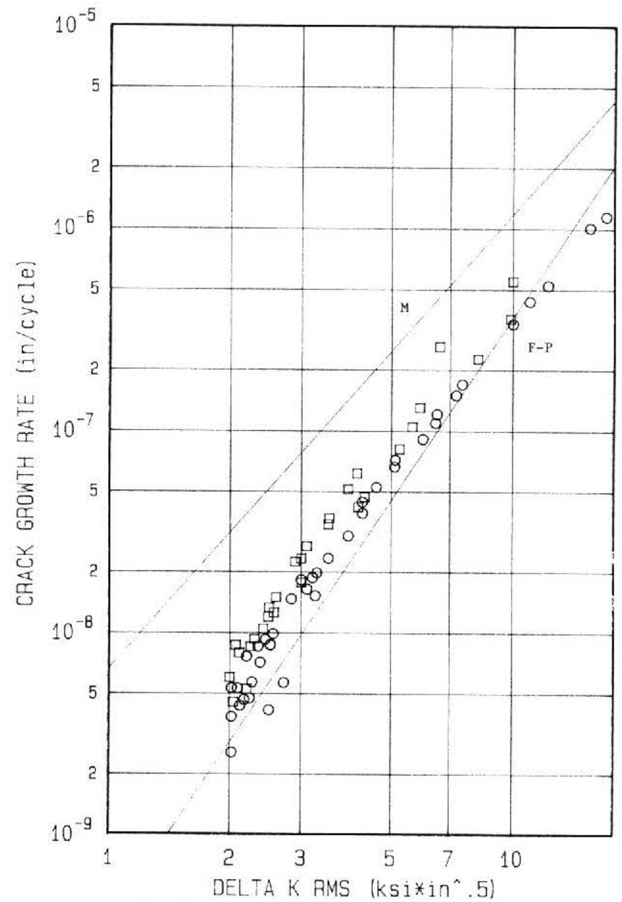

Fig. C-4. Fatigue crack growth rate measurements on two specimens of M244 steel.

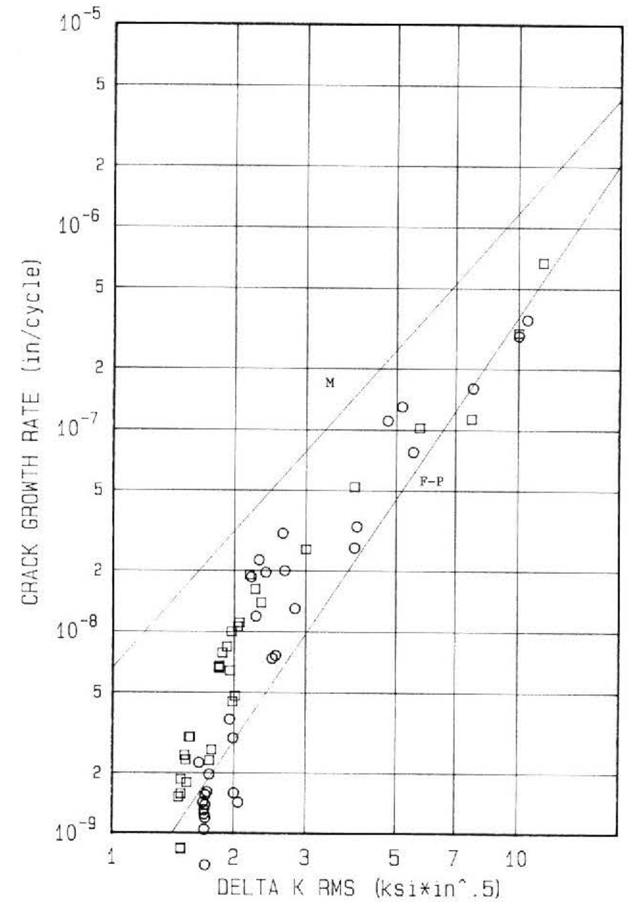

Fig. C-5. Fatigue crack growth rate measurements on two specimens of M222 steel.

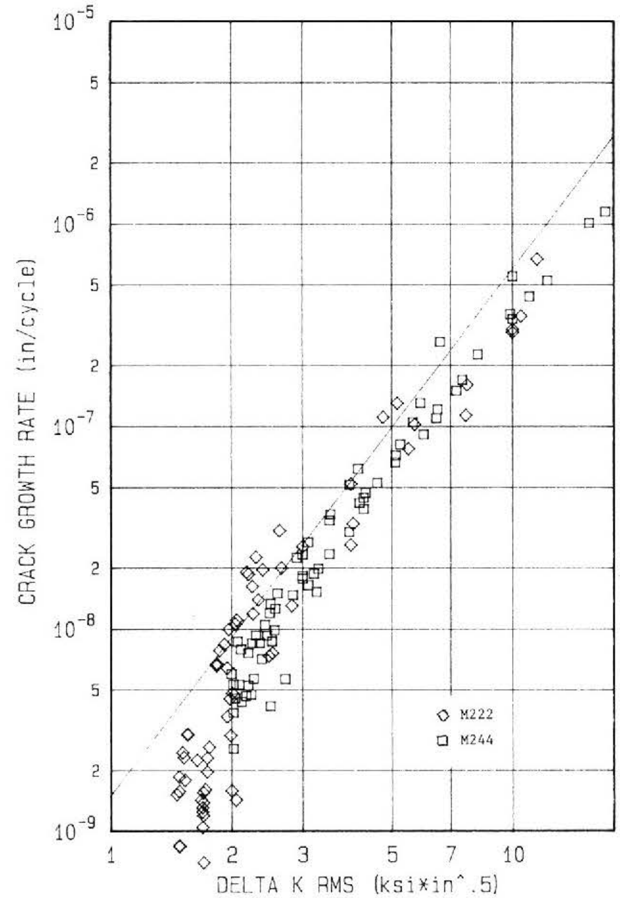

Fig. C-6. Fatigue crack growth rate measurements on M222 and M244 steel.

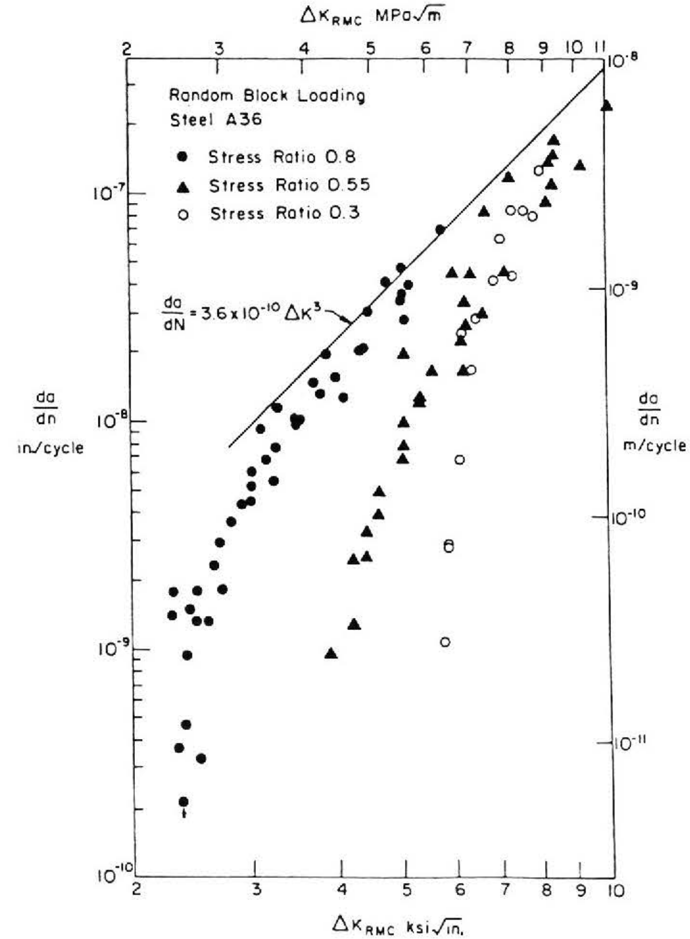

Fig. C-7. Fatigue crack growth test data from Fisher, et al [3].

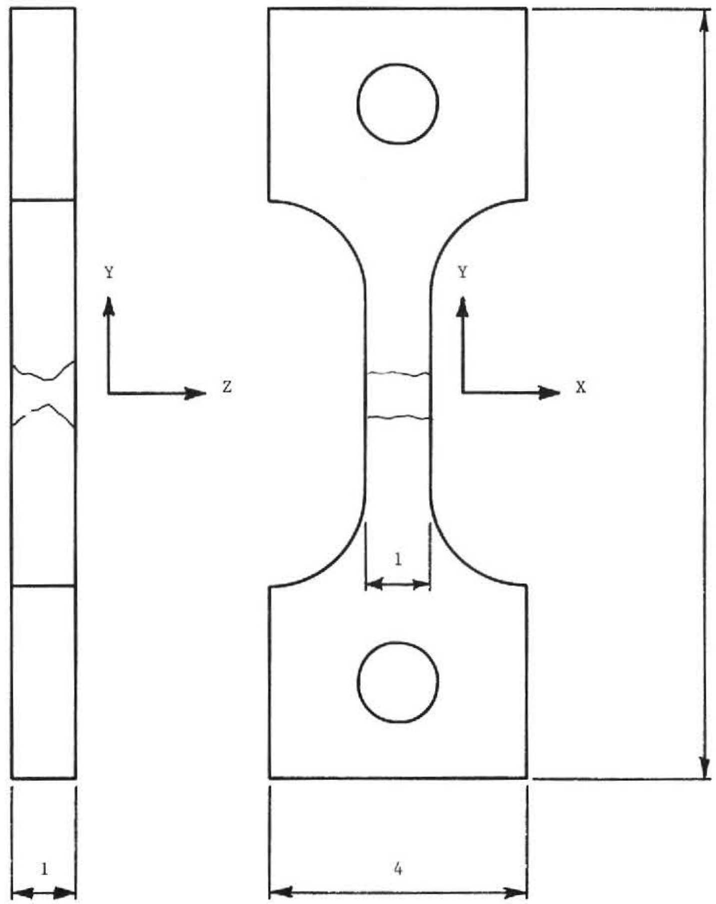

Fig. C-8. Axial fatigue specimen used to test welds with deliberately introduced imperfections. (Dimensions in inches.)

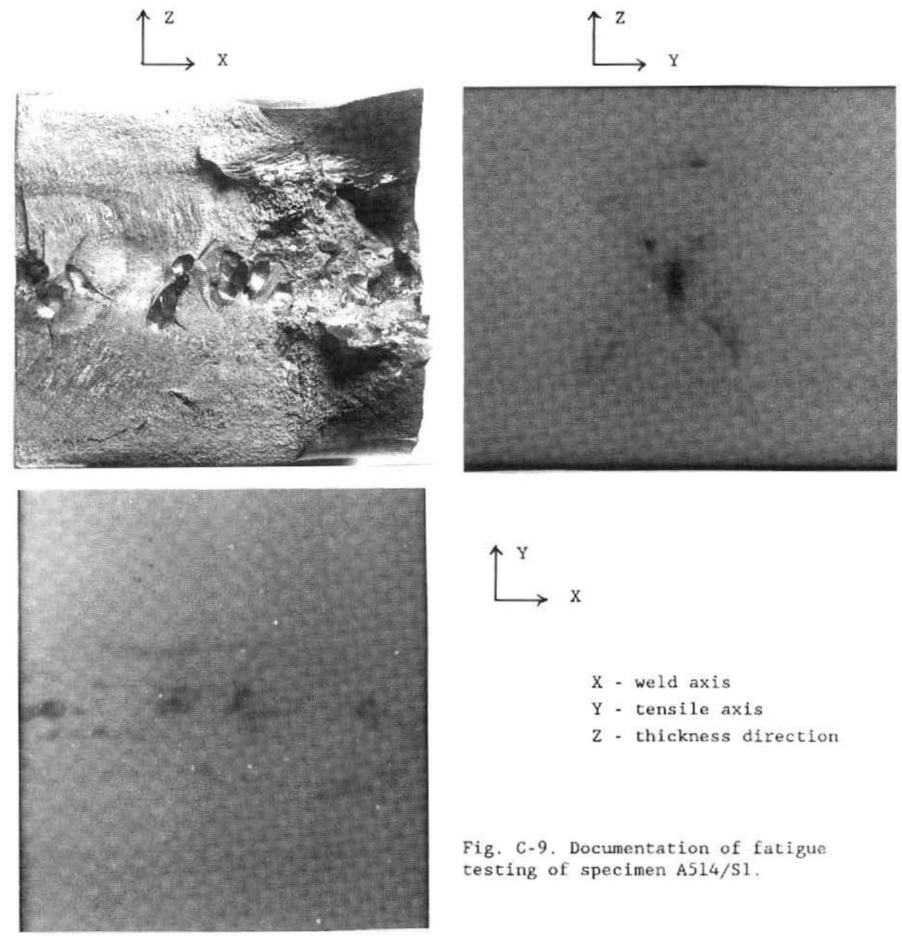

Fig. C-9. Documentation of fatigue testing of specimen A514/S1.

Specimen failed after 29.59 million load cycles at $\Delta\sigma_{rms}$ of 6.5 ksi. Fatigue cracking started from cluster of three imperfections at left. The cluster has an effective diameter of about 0.15 inch, which gives an initial ΔK_{rms} of 3.2 ksi$\sqrt{in}$. Other imperfections visible on the fracture surface were not fatigue origins.

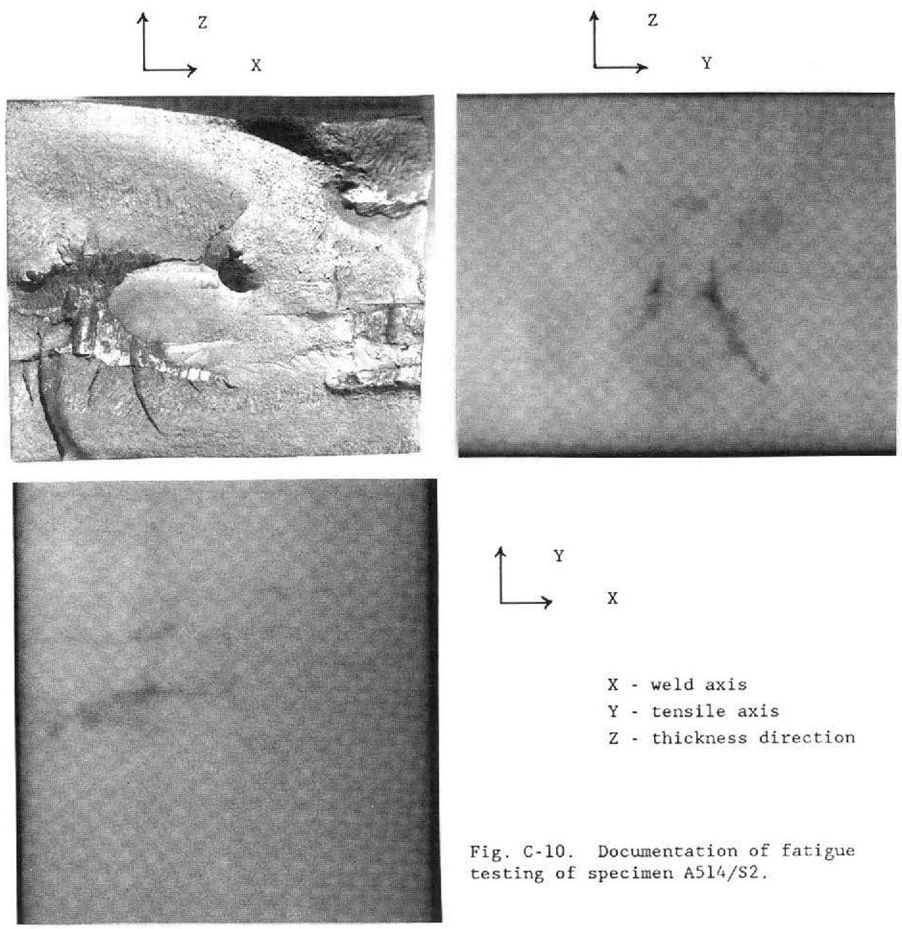

X - weld axis
Y - tensile axis
Z - thickness direction

Fig. C-10. Documentation of fatigue testing of specimen A514/S2.

Specimen failed after 25 million load cycles at $\Delta\sigma_{rms}$ of 5.5 ksi. The dominant imperfection, visible on the left side of the fracture surface, was the fatigue origin. It had an effective width of 0.28 inch giving an initial ΔK_{rms} of about 3.7 ksi$\sqrt{\text{in}}$.

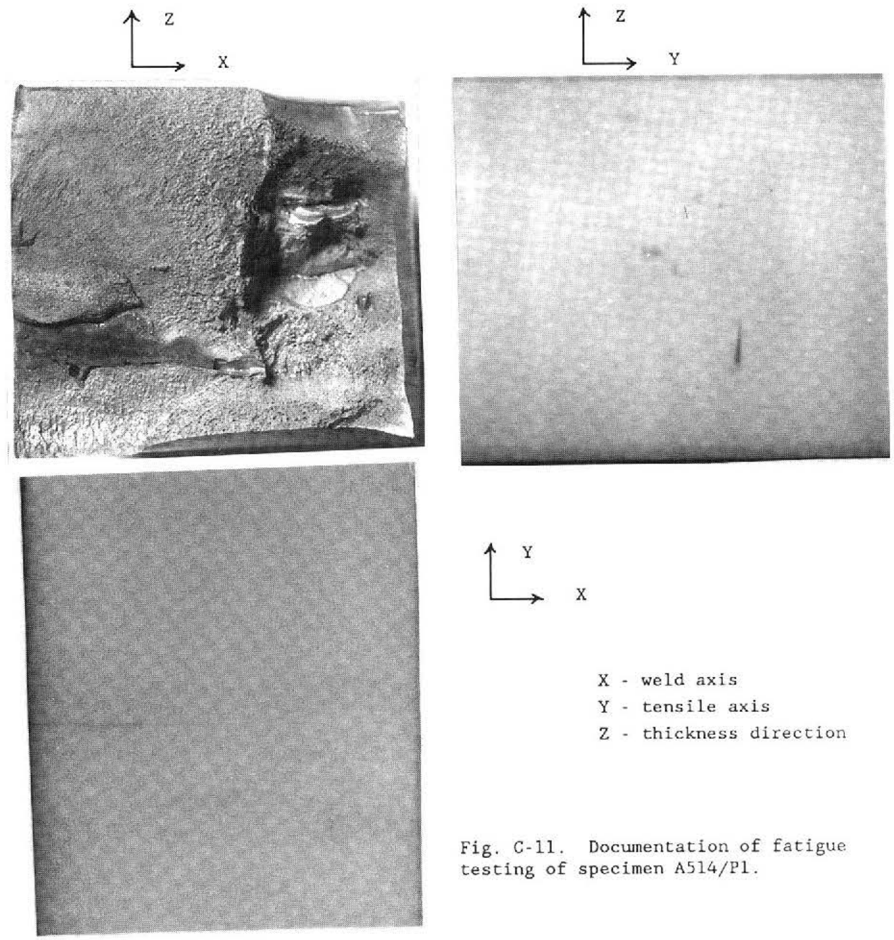

X - weld axis
Y - tensile axis
Z - thickness direction

Fig. C-11. Documentation of fatigue testing of specimen A514/P1.

Specimen had not failed after 29.59 million load cycles at $\Delta\sigma_{rms}$ of 6.5 ksi and an additional 9.57 million cycles at $\Delta\sigma_{rms}$ of 9.5 ksi. Specimen was broken open by fatigue cycling for 1.47 million cycles at a constant stress amplitude of 27 ksi. A large planar imperfection is visible in the radiographs, and it can be seen on the fracture surface extending in from the left-hand edge about one-quarter of the way from the bottom. Beach marks on the fracture surface indicate, however, that the fatigue cracking did not start from this large imperfection, but from a smaller one near the mid-point of the left-hand edge. This imperfection was about 0.030 inch across corresponding to an initial ΔK_{rms} = 2.8 ksi$\sqrt{\text{in}}$.

Z
X

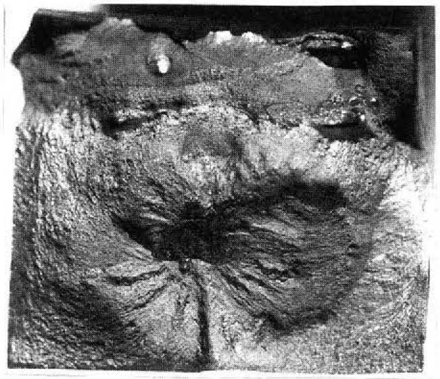

Z
Y

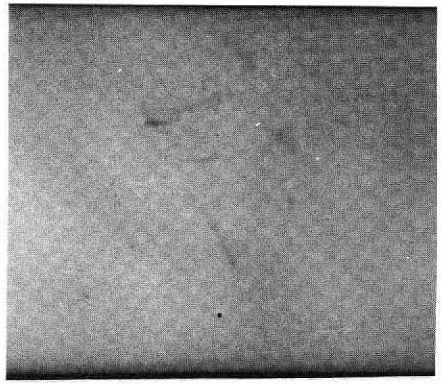

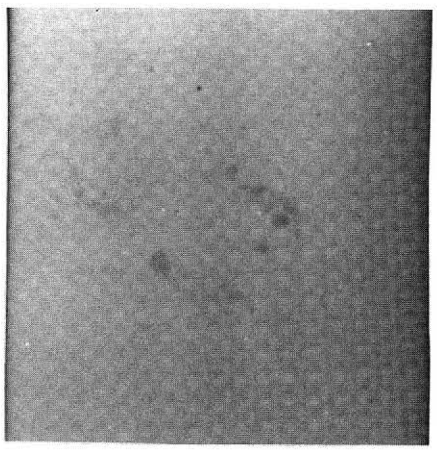

Y
X

X - weld axis
Y - tensile axis
Z - thickness direction

Fig. C-12. Documentation of fatigue testing of specimen A514/P2.

The fracture surface reveals an imperfection near the center of the specimen approximately 0.2 by 0.3 inch in size. Absence of beach marks suggests that fatigue had not initiated after 33.78 million cycles at $\Delta\sigma_{rms}$ = 6.5 ksi, but that all the cracking occurred only in the final constant amplitude cycling at 27 ksi.

Z
X

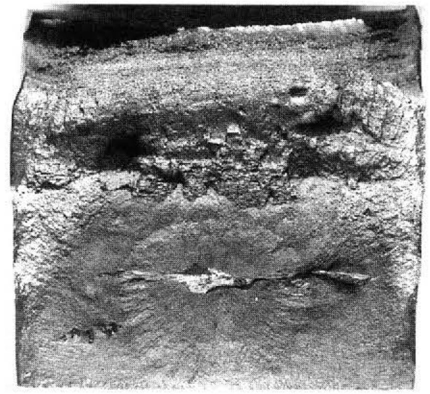

Z
Y

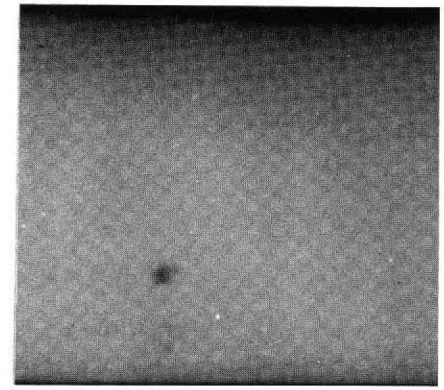

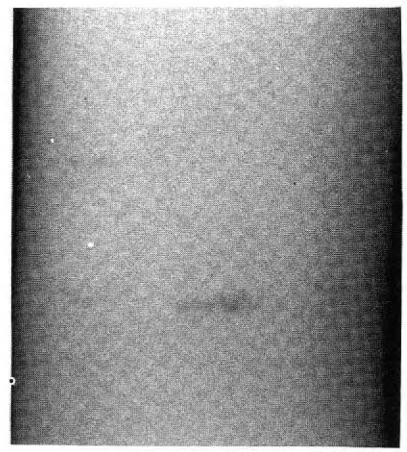

Y
X

X - weld axis
Y - tensile axis
Z - thickness direction

Fig. C-13. Documentation of fatigue testing of specimen A588/A.

The fracture surface reveals a central imperfection about 0.06 inch across. Beach marks indicate that this was the origin of the fatigue failure and that cracking had occurred during 51.3 million variable amplitude cycles at $\Delta\sigma_{rms}$ = 8 ksi. This corresponds to an initial ΔK_{rms} = 2.5 ksi$\sqrt{}$in.

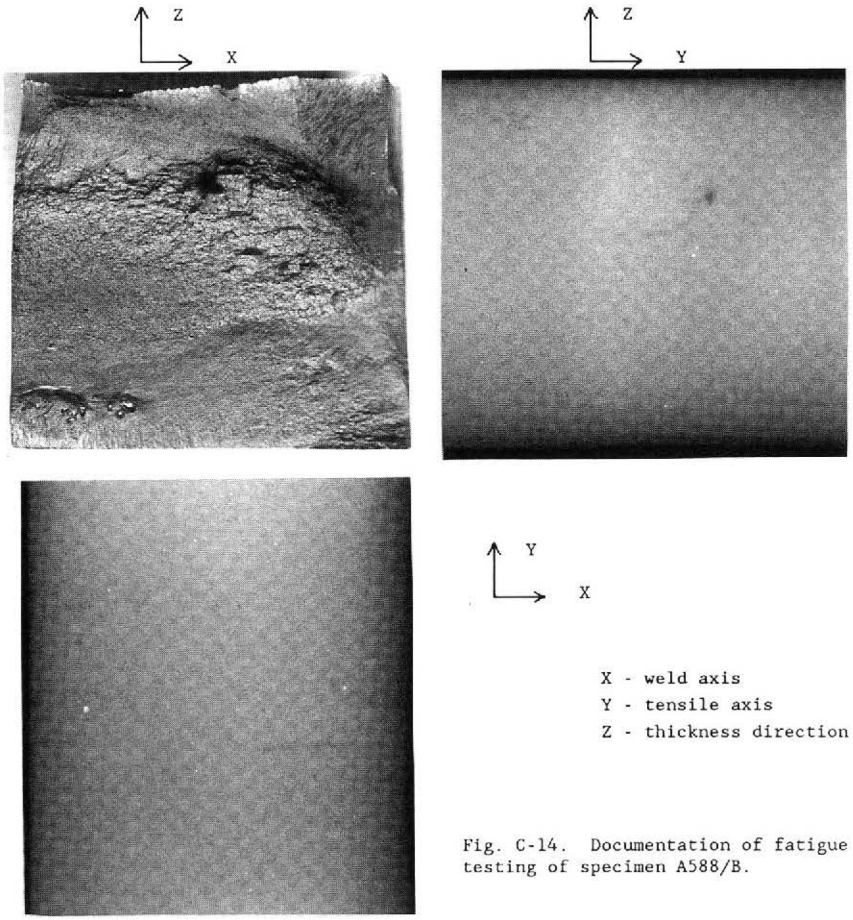

Fig. C-14. Documentation of fatigue testing of specimen A588/B.

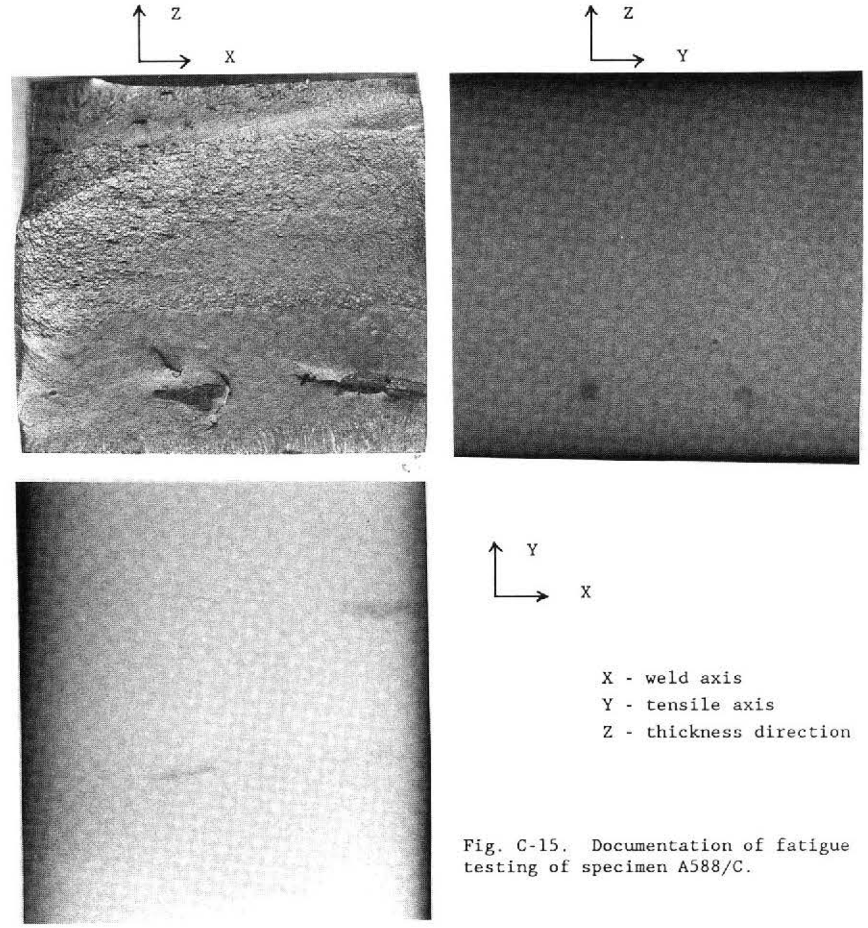

Fig. C-15. Documentation of fatigue testing of specimen A588/C.

Fracture origin is an imperfection near one corner (lower left) of the fracture surface. Beach marks indicate cracking during the variable amplitude loading, 52.25 million cycles at $\Delta\sigma_{rms}$ = 8 ksi. Estimated effective size of imperfection is 0.1 inch which provided an initial ΔK_{rms} = 3.2 ksi$\sqrt{in}$.

The specimen failed after 7 million cycles of variable amplitude loading at $\Delta\sigma_{rms}$ = 8 ksi. The fracture surface contains two elongated imperfections, both of which appear to have been fatigue origins. They each have a width of about 0.05 inch which corresponds to an initial ΔK_{rms} of about 2.25 ksi$\sqrt{in}$.

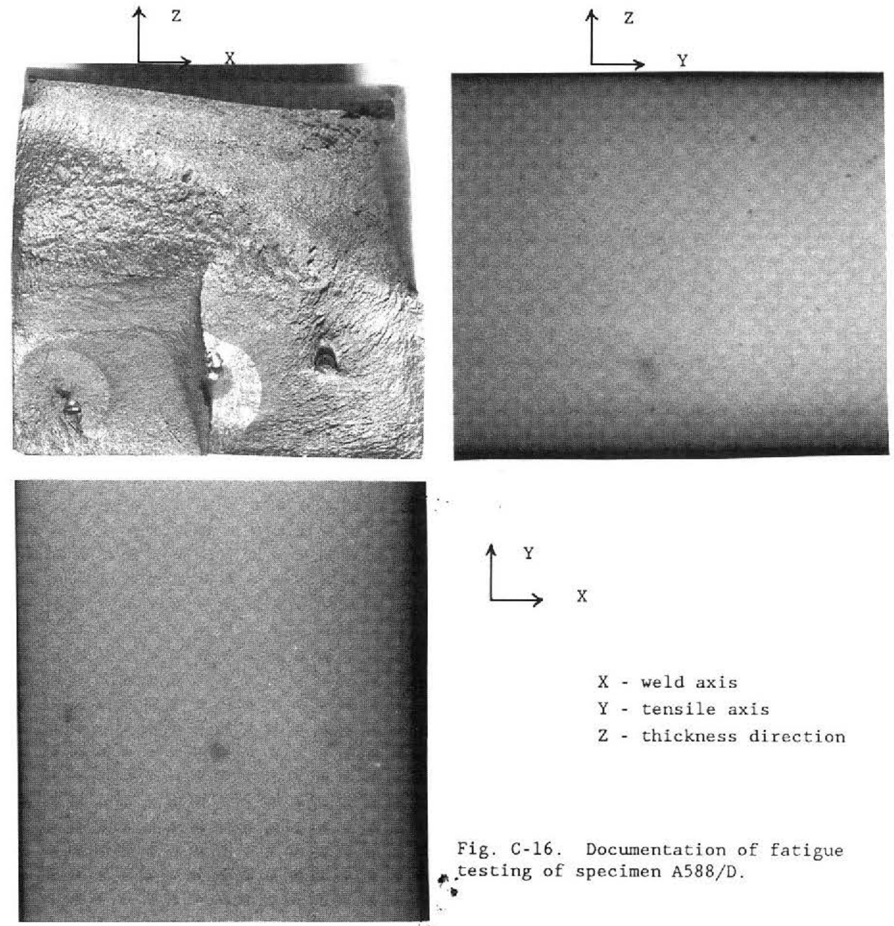

Fig. C-16. Documentation of fatigue testing of specimen A588/D.

The fracture plane contains three distinct, isolated imperfections all of about the same size, approximately 0.05 inch across. Two appear to be fatigue origins and show clear evidence of crack growth in the initial variable amplitude loading, 50.5 million cycles at $\Delta\sigma_{rms}$ of 8 ksi. The third does not appear to have been a fatigue origin. Imperfection size corresponds to an initial ΔK_{rms} of about 2.25 ksi$\sqrt{in.}$